arXiv:hep-ph/9611217v1 3 Nov 1996

OHSTPY-HEP-T-96-026
CERN-TH/96-316
DESY 96-226

A Global χ^2 Analysis of Electroweak Data in SO(10) SUSY GUTs

Tomáš Blažek[a*], Marcela Carena[b,c], Stuart Raby[a†] and Carlos E.M. Wagner[b]

[a] *Department of Physics, The Ohio State University, 174 W. 18th Ave., Columbus, OH 43210*

[b] *Theory Division, CERN, Geneva, Switzerland*

[c] *Deutsches Elektronen-Synchrotron, Hamburg, Germany*

November 1, 1996

Abstract

We present the details of a global χ^2 analysis of electroweak data, including fermion masses and mixing angles, in SO(10) SUSY GUTs. Just as precision electroweak data is used to test the Standard Model, the well determined Standard Model parameters are the precision electroweak data for testing theories beyond the Standard Model. In this paper we use the latest experimentally measured values for these parameters. We study several models discussed in the literature. One of these models provides an excellent fit to the low energy data with $\chi^2 \sim 1$ for 3 degrees of freedom. We present graphs of constant χ^2 contours as functions of position in soft SUSY breaking parameter space, as well as our predictions for a few selected points in parameter space. We also study the sensitivity of our results to changes in various parameters. Finally, we discuss the consequences of our work in the context of a general MSSM analysis at the Z scale.

PACS numbers: 12.15.Ff, 12.15.Hh, 12.60.Jv

[*] On leave of absence from the Dept. of Theoretical Physics, Comenius Univ., Bratislava, Slovakia; blazek@mps.ohio-state.edu

[†] raby@mps.ohio-state.edu

1 Introduction

The Standard Model is by far one of the greatest achievements of the twentieth century. Its stature is further elevated by the fact that after a decade or more of testing there is still no evidence for physics beyond the Standard Model(SM). Yet we nevertheless remain firm in our belief that the SM cannot be the whole story. For one thing there are 18 phenomenological parameters which await derivation from a more fundamental theory. In particular 13 of these parameters are related to the fermion mass sector. Secondly, there is growing evidence that neutrinos may have mass; yet another indication of physics beyond the SM. Finally, a quantum theory of gravity has yet to be incorporated into the SM. Clearly string theory is the leading candidate for a fundamental theory of Nature; it can incorporate gravity, as well as the known quarks, leptons and gauge interactions. The problem lies in finding the matching conditions between this fundamental string theory and the effective field theory which describes the physics below the Planck (or string) scale.[1]

The fermion mass sector is now well measured. It is clear that fermions come in well defined families with an amazingly simple regularity in the hierarchy of masses and mixing angles. It is hoped that by understanding this sector we can find the correct matching conditions at the string scale. Now seems an appropriate time to begin such an endeavor. It was only ten years ago that the top quark mass and the CKM angle V_{ub} were unknown; while V_{cb} and the weak mixing angle $sin^2\theta_W$ were measured, but with large error bars. Today, as a result of both experimental and theoretical progress, all but one of the 18 parameters of the Standard Model are known to much better accuracy [the Higgs mass has yet to be measured]. These parameters are the precision electroweak data for testing theories of fermion masses.

Of course once setting out to test theories of fermion masses, we must necessarily choose some particular theories to test. It is in this choice of a theory that we now invoke some theoretical prejudices. It seems clear to us that the simple observed pattern of fermion masses and mixing angles is not due to some *random* dynamics at an effective cut-off scale M but is instead evidence that a small set of fermion mass operators are dominant. Thus we are lead to postulate –

1. that a few effective operators at an effective cut-off scale M (where $M = M_{Planck}$ or M_{string}) (or at a GUT scale M_G) dominate the quantitative behavior of fermion masses and mixing angles; and

2. that a more fundamental theory, incorporating Planck or stringy dynamics, will generate an effective field theory below M including these dominant operators.

We are thus encouraged to find this effective field theory, thereby determining the matching conditions near the Planck scale. However, in order to make progress, it is clear that

[1] Within string theory the problem is different; it is to understand string dynamics and why one particular vacuum is preferred over all others.

order of magnitude comparisons with the data are insufficient. Moreover, since the predictions of any simple theory are correlated, a *significant test* of any theory requires a *global fit to all the low energy data*. This paper makes the first attempt to bring the tests of theories of fermion masses into conformity with the accuracy of the low energy data.

In this paper we present a global χ^2 analysis of precision electroweak data, *including fermion masses and mixing angles*, within the context of several theories of fermion masses based on SO(10) SUSY GUTs. Of course, the self-consistent global analysis we describe can be applied to any predictive theory.

Why look at SO(10) SUSY GUTs?

- We use SUSY GUTs since they give the simplest explanation for the experimental observation that the three gauge couplings appear to meet at a scale of order 10^{16} GeV[1].

- We use SO(10) since it provides the simplest explanation for the observed family structure of the light fermions[2].

An important feature of our analysis is the inclusion of low energy supersymmetric threshold corrections. We study their significance for minimizing χ^2. As has been shown earlier [3][4], with $\tan\beta$ large there are potentially large corrections to those observables which are $\tan\beta$ suppressed at tree level. These observables include, for instance, masses of b, s and d quarks, and masses of charged leptons. The CKM elements V_{cb} and V_{ub}, resulting from the mismatch between up- and down-type quark mass matrices, also get these corrections. In this case the large corrections to the d-quark mass matrix are passed on to the unitary matrices which diagonalize it [4]. All these corrections could potentially conspire and open a window in parameter space which has been unnoticed in the analysis neglecting them. In fact, such interplay is hard to study in the usual bottom-up scenario, but simple to implement in a global top-down analysis like this one.

In section 2 we describe the low energy observables which enter the χ^2 analysis, their measured values and the associated experimental and/or theoretical errors.

In section 3 we discuss the self-consistent evaluation of the theoretical predictions, starting with the effective SO(10) GUT and the resulting boundary conditions at M_G; then detailing the renormalization group running to M_Z and the threshold corrections included at the weak scale.

In section 4 we discuss models with four effective mass operators at the GUT scale. We show in detail results for the best model out of nine ADHRS[5] models. In this model [model 4] the number of arbitrary Yukawa parameters $n_y = 5$. The best fits give $\chi^2 \sim 13 - 14$ for 5 degrees of freedom. All low energy observables are fit to within their 2σ bounds. The fits for 4 observables, however, (V_{cb}, V_{ub}/V_{cb}, the Kaplan-Manohar-Leutwyler ellipse parameter Q and the Jarlskog CP violating invariant J) lie close to the 2σ border. We show that these results are true predictions of the theory, i.e. we see no other way to improve the results,

except with the addition of a new operator contributing to the 13 and 31 elements of the Yukawa matrices [2].

In section 5 we analyze 3 models derived from complete SUSY GUTs discussed recently by Lucas and S.R.[7]. One of these three models is identical to model 4 of ADHRS when states with mass greater than M_G are integrated out; this is model 4b. The other two include one new effective operator at the GUT scale which distinguishes the two models, 4a and 4c. We find that model 4a gives a best fit with $\chi^2 \sim 3$ for 3 dof in a small corner of parameter space, while model 4c gives $\chi^2 \leq 1$ for 3 dof over a large subspace of the allowed parameter space.

Our main results are found in figures [1 - 4] and tables (III - IX). These include graphs of constant χ^2 contours in the two dimensional soft SUSY parameter space labelled by m_0, a universal squark and slepton mass parameter, and $M_{1/2}$, a universal gaugino mass parameter both with values given at M_G. We have several such plots for different values of the Higgs mass parameter μ, given at M_Z. In the tables we give the computed values for the low energy observables for a few selected points in parameter space. We also include values for the Higgs and SUSY spectra, the CP violating angles $\alpha,\ \beta$ and γ, measurable in neutral B decays, the Wolfenstein parameters $\eta,\ \rho$, and the ratio m_u/m_d for these points. Note, in figure 5, we present a scatter plot for values of $(\sin 2\alpha,\ \sin 2\beta)$ predicted by models 4a and 4c for points in figures 3(a - c) and 4(a - c), respectively, with χ^2 values ≤ 3. Finally we test the sensitivity of χ^2 to changes in various parameters.

Section 6 contains further discussion of our results and conclusions.

2 Low energy observables – experimental values

Our χ^2 function includes 20 low energy observables. In addition we have incorporated the experimental bounds on sparticle masses into the code as a penalty in χ^2; added if one of these bounds is violated. This gaurantees that we remain in the experimentally allowed regions of parameter space. Let us now discuss the experimental observables and their errors.

We have

- 6 parameters associated with the Standard Model gauge and electroweak symmetry breaking sectors — $\alpha_s(M_Z),\ \alpha_{EM},\ G_\mu,\ M_W,\ M_Z,$ and ρ_{new};
- 13 parameters associated with fermion masses and mixing angles — $M_t,\ m_b(M_b),\ (M_b - M_c),\ m_s,\ m_d/m_s,\ Q^{-2},\ M_\tau,\ M_\mu,\ M_e,\ V_{us},\ V_{cb},\ V_{ub}/V_{cb},$ and J ;[3] and
- the branching ratio for $b \to s\gamma$,

[2]Note that models with smaller values of $\tan\beta$ not only involve an extra free parameter but also require additional operators to correctly reproduce the experimental values for the first generation quark masses [6].

[3]In the actual χ^2 analysis J is replaced by the hadronic matrix element $\hat{B}_K$ as will be explained later in this section.

where ρ_{new} includes the added contribution to the electroweak ρ parameter from new physics beyond the SM, Q is the Kaplan-Manohar-Leutwyler ellipse parameter[8] relating u, d, and s quark masses and J is the Jarlskog CP violating invariant[9] (see more on these parameters below). Note also, that mass parameters denoted with a capital letter M are defined as pole masses, while $m_b,\ m_s,\ m_d,\ m_u$ are defined as the $\overline{MS}$ running masses. The three light quark running masses are evaluated at the scale 1 GeV.

The experimental values for the observables are given in table 1 with the associated experimental or theoretical error σ. *Note, σ is taken to be either the experimental error or 1/2%, whichever is larger.* This is because our theoretical calculation also introduces an error; the numerical solution to the renormalization group equations is computed with some limited precision and the values of all observables are calculated within the first orders of the perturbative expansion in couplings. Thus 1/2% represents a conservative simple estimate of the combined theoretical error assigned to each low energy theoretical output [4]. As a consequence, the listed errors for $M_Z,\ M_W,\ G_\mu,\ \alpha_{EM},\ M_\tau,\ M_\mu,\ M_e$ are dominated by theoretical uncertainties.

For $\alpha_s(M_Z)$ we use the central value quoted by Schmelling in Warsaw[10]. However, for the error we choose a conservative value as suggested by Webber[11] or Burrows[12]. This accounts for the fact that the systematic errors of individual α_s measurements are significant and thus caution is required when adding them together.

Note that the traditional Standard Model parameter $\sin^2\theta_W(M_Z)|_{\overline{MS}}$ is not among the observables in table 1. Neither is J, ϵ_K or any other standard CP violating quantity listed. Instead, in the list of observables, $\sin^2\theta_W(M_Z)$ is replaced by the Fermi constant G_μ, and J is replaced by the bag constant $\hat{B}_K$. G_μ is substituted for $\sin^2\theta_W(M_Z)$ since the former is extracted from the muon lifetime formula [13] with very little sensitivity to the particle content at the scale M_Z and the underlying theory at this scale. In fact, it could be defined completely in the context of the effective four-fermi contact interaction plus electromagnetism, and the remaining uncertainty of the order M_μ^2/M_W^2 would then appear in the quantities derived from G_μ. On the contrary, the experimental value of $\sin^2\theta_W(M_Z)$ in the $\overline{MS}$ scheme is derived from the precision measurements at the Z peak. Loop effects play an important role in its precise determination and hence one has to specify the theory at M_Z and its particle content, and then calculate all relevant radiative corrections. Thus the underlying theory is an explicit input for the extraction of the experimental value of $\sin^2\theta_W(M_Z)$ and, naturally, it is commonly taken to be the Standard Model (SM). However, we adopt an approach where the minimal supersymmetric extension of the Standard Model (MSSM) is matched directly to the low energy $SU(3)_c\times U(1)_{em}$ effective theory by integrating out the superpartners at the same time as the top quark and W/Z bosons (at a single scale M_Z); hence there is no room for the SM. This approach is particularly sensible if there are light SUSY particles (below M_Z), such as charginos, neutralinos, pseudoscalar Higgs, etc.,

[4]For G_μ we take σ to be 1%. This is to account for the additional error resulting from our neglecting one loop SUSY box and vertex corrections.

for then there is no energy regime where the SM dominates[14]. Although not among the observables contributing to the χ^2 function, the SM value of $\sin^2\theta_W(M_Z)$ is displayed among the model predictions in tables 8 and 9.

The CP violating parameter J is defined by the expression –

$$J = Im(V_{ud}V_{ub}^*V_{cb}V_{cd}^*) \approx |V_{cd}||V_{ub}/V_{cb}||V_{cb}|^2 \ \sin\xi \tag{1}$$

where ξ is the CP violating phase. We test J by a comparison to the experimental value extracted from the well-known $K^0 - \overline{K^0}$ mixing observable $\epsilon_K = (2.26 \pm 0.02) \times 10^{-3}$. The largest uncertainty in such a comparison, however, comes in the value of the QCD bag constant $\hat{B}_K$. We thus exchange the Jarlskog parameter J for $\hat{B}_K$ in the list of low-energy data we are fitting. Our theoretical value of $\hat{B}_K$ is defined as that value needed to agree with ϵ_K for a set of fermion masses and mixing angles derived from the GUT-scale. We test this theoretical value against the "experimental" value of $\hat{B}_K$, which is given in table 1. This value, together with its error estimate, is obtained from recent lattice calculations[15].

The experimental value for ρ_{new} is obtained from Langacker's combined fits to the precision electroweak data, presented at recent workshops[16].

For fermion masses and mixing angles we use those combinations of parameters which are known to have the least theoretical and/or experimental uncertainties. For example, while the bottom and top quark masses are known reasonably well, the charm quark mass is not known as accurately. On the other hand, heavy quark effective theory relates the mass difference $M_b - M_c$ between the bottom and charm quark *pole masses* to about 5% accuracy[17]. We thus use this relation, instead of the charm quark mass itself, to test the theory. We note that M_b and M_c are calculated from the $\overline{MS}$ running masses, $m_b(M_b)$ and $m_c(M_c)$ using two loop QCD threshold corrections. In fact there are infra-red renormalons which make this perturbative evaluation ambiguous. However, these renormalon contributions cancel in the mass difference. Moreover, it has been argued that this ambiguity cancels when extracting V_{cb} via semileptonic B decays[17][18].[5]

Similarly, among the three light quarks there is one good relation, (reparametrization invariant and free of $O(m_q)$ corrections) which severely constrains any theory of fermion masses. This is the Kaplan-Manohar-Leutwyler ellipse given by

$$1 = \frac{1}{Q^2}\frac{m_s^2}{m_d^2} + \frac{m_u^2}{m_d^2} \tag{2}$$

or

$$Q = \frac{\frac{m_s}{m_d}}{\sqrt{1 - \frac{m_u^2}{m_d^2}}} \tag{3}$$

[5]The correction to the bottom mass $(M_b - m_b(M_b))/m_b(M_b)$ *at two loops* is $\approx 25\%$ less than the results found recently by Ball, Beneke and Braun using an infinite order resummation within a naive non-abelianization of the mass correction[18]. The theoretical error for this result is also estimated to be about 25%. By using two loop pole masses, combined with the mass relation for $M_b - M_c$, we obtain a small value for $m_c(M_c)$. This value increases when using the scheme of BBB[18].

where Q is the ellipse parameter. The experimental value for Q is obtained from a weighted average of lattice results and a chiral Lagrangian analysis, with significant contributions from the violation of Dashen's theorem[19]. We follow Donoghue[20] and assign a conservative 10% error to the experimental value of Q^{-2}. Note that m_d/m_s derived from chiral Lagrangian analysis is not free of first order quark mass corrections, and hence σ is much smaller for Q^{-2} than for m_d/m_s[20]. In addition, we do not constrain m_u/m_d independently, as suggested by Leutwyler[21], which requires additional input from an expansion in $1/N_{color}$. Instead we quote values for m_u/m_d as output. Finally we use m_s given by the PDG[22]. At the end of section V we consider the lower values for m_s suggested by recent lattice calculations[25].

The remaining parameters are more or less self evident. We just remark that the central value for V_{cb}, as well as the error bars, has steadily decreased in the last 5 years, making it a very significant constraint.[6] In addition, the value for V_{ub}/V_{cb} changed dramatically in 1992. It changed from approximately 0.15 ± 0.05 to its present value 0.08 ± 0.02, where the errors were and continue to be dominated by theoretical model dependence. Clearly the systematic uncertainties were large but are now hopefully under control.

3 Low energy observables – computed values

In our analysis we consider the minimal supersymmetric standard model defined at a GUT scale M_G with, in all cases (but one), tree level GUT boundary conditions on gauge couplings and Yukawa matrices. In this one case, we include an arbitrary parameter, ϵ_3, given by

$$\epsilon_3 \equiv \frac{\alpha_3(M_G) - \tilde{\alpha}_G}{\tilde{\alpha}_G} \quad \text{with} \quad \tilde{\alpha}_G \equiv \alpha_1(M_G) = \alpha_2(M_G) \tag{4}$$

which parametrizes the one loop threshold correction to gauge coupling unification.[7] We also include 7 soft SUSY breaking parameters — an overall scalar mass m_0 for squarks and sleptons, a common gaugino mass $M_{1/2}$, the parameters A_0, B and μ, and in addition we have allowed for non-universal Higgs masses, m_{H_u} and m_{H_d}.[8] Thus the number of arbitrary

[6] Note, the actual value of V_{cb} is correlated with the values of m_b and m_c[17]. We have not included this correlation in our analysis.

[7] ϵ_3 is calculable in any complete SUSY GUT. It is also constrained somewhat by the bounds on the nucleon lifetime[7].

[8] Note that if the messenger scale of SUSY breaking is M_{Planck} then our analysis is not completely self-consistent. In any complete SUSY GUT defined up to an effective cut-off scale $M > M_G$, the interactions above M_G will renormalize the soft breaking parameters. This will, in general, split the degeneracy of squark and slepton masses at M_G even if they are degenerate at M. On the other hand, bounds on flavor changing neutral current processes, severely constrain the magnitude of possible splitting. Thus these corrections must be small. In addition, in theories where SUSY breaking is mediated by gauge exchanges with a messenger scale below (but near) M_G, the present analysis is expected to apply unchanged, since in this case squarks and sleptons will be nearly degenerate at the messenger scale. The Higgs mases, on the other hand, are

parameters in the effective GUT includes the 3 gauge parameters, 7 soft SUSY breaking parameters and n_y Yukawa parameters. The number n_y and the form of the Yukawa matrices are model dependent. The models are discussed in sections IV and V.

The effective theory between M_G and M_Z is the MSSM. We use two loop SUSY renormalization group equations [RGE] for dimensionless parameters and one loop RGE for dimensionful parameters from M_G to M_Z. However we have checked that the corrections to our results obtained by using two loop RGE for dimensionful parameters[26] are insignificant. When in the framework of the MSSM we use Dimensional Reduction regularization in the Modified Minimal Subtraction Scheme. This renormalization procedure will be abbreviated as $\overline{DR}$ in the following text.

When crossing the M_Z scale we match the MSSM to the non-supersymmetric $SU(3)_c \times U(1)_{em}$ gauge theory, i.e. our effective theory below the Z threshold is standard QCD and electromagnetism. In this effective theory we perform the calculations using Dimensional Regularization in the Modified Minimal Subtraction scheme. Quantities renormalized according to this prescription will appear with a standard subscript $\overline{MS}$ in the following formulas. Below the Z scale, three loop QCD renormalization group equations run quark masses and α_s down to lower scales. When this running crosses the b and c mass thresholds the number of flavors is reduced by one each time. Finally we end up with the three flavor QCD RGE as we arrive at the scale of $1\,GeV$, where the three light quark masses are evaluated. In addition, QED running is included to one loop precision. (For further details see [27].)

At M_Z we calculate complete one loop MSSM corrections to the W and Z masses. Thus the W and Z pole masses are given by the formulae:

$$M_W^2 = \frac{1}{4}\, g_2^2\, v^2 + \delta M_W^2, \tag{5}$$

$$M_Z^2 = \frac{1}{4}\, (\frac{3}{5}\, g_1^2 + g_2^2)\, v^2 + \delta M_Z^2, \tag{6}$$

where δM_W^2 and δM_Z^2 are the complete one loop self-energies [14],[28] in the $\overline{DR}$ scheme and g_1, g_2 are the $\overline{DR}$ gauge couplings evaluated at M_Z in the MSSM.

The Higgs vacuum expectation value v is an implicit function of soft SUSY breaking parameters and gauge and Yukawa couplings. It is determined by self consistently demanding minimization of the tree level Higgs potential. The actual value for v is found by minimizing χ^2.

The theoretical value of G_μ is calculated according to the formula

$$G_\mu = \frac{\pi\, \alpha(M_Z)}{\sqrt{2} M_W^2\, \sin^2\theta_W(M_Z)}\, \frac{1}{1 - \Delta\hat{r}_W^{MSSM}}. \tag{7}$$

probably dominated by new interactions which also generate a μ term. It is thus plausible to expect the Higgs masses to be split and independent of squark and slepton masses. The parameter A_0 could also be universal at the messenger scale.

The right-hand side of this equation is consistently evaluated in the $\overline{DR}$ scheme within the context of the MSSM. The electromagnetic structure constant α and $\sin^2\theta_W$ are determined by the relations among the gauge coupling constants α_1 and α_2:

$$\sin^2\theta_W(M_Z) = \frac{\frac{3}{5}\alpha_1(M_Z)}{\frac{3}{5}\alpha_1(M_Z)+\alpha_2(M_Z)}, \tag{8}$$

$$\alpha(M_Z) = \alpha_2(M_Z)\,\sin^2\theta_W(M_Z)\,. \tag{9}$$

$\Delta\hat{r}_W^{MSSM}$ in (7) contains the corrections from the W self-energy and vertex and box diagrams. We follow refs. ([14],[29]) closely, but not to all details: we don't include the vertex and box diagrams containing SUSY particles. These have a minor effect (see results in [14]) and we compensate for them with an additional 1/2% error on G_μ, as already mentioned in a previous footnote. In fact, we use a reverse procedure to the one introduced in [14], where the equation (7) is utilized to derive the MSSM value of $\sin^2\theta_W$ in the bottom-up approach starting from the precise value of G_μ.

When crossing the Z threshold, gauge couplings are subject to two different kinds of corrections. That is to account for the states which are integrated out at this scale , and for the transition from the $\overline{DR}$ scheme to the $\overline{MS}$ scheme. First, when the SUSY particles, the top quark and the Z and W gauge bosons are integrated out , the threshold corrections to $\alpha_s|_{\overline{DR}}$ and $\alpha|_{\overline{DR}}$ read

$$\frac{\delta\alpha_s}{\alpha_s} = \frac{\alpha_s}{\pi}\quad\Big(\quad\frac{1}{12}\sum_{\substack{i=1\\(\,all\\squarks)}}^{12}\log\frac{m_{\tilde{q}_i}}{M_Z}+\log\frac{M_{\tilde{g}}}{M_Z}+\frac{1}{3}\log\frac{M_t}{M_Z}\Big), \tag{10}$$

$$\begin{aligned}\frac{\delta\alpha}{\alpha} = \frac{\alpha}{2\pi}\quad\Big(\quad&\frac{4}{9}\sum_{\substack{i=1\\(\,\mathrm{u-}type\\squarks)}}^{6}\log\frac{m_{\tilde{q}_i}}{M_Z}+\frac{1}{9}\sum_{\substack{i=1\\(\,\mathrm{d-}type\\squarks)}}^{6}\log\frac{m_{\tilde{q}_i}}{M_Z}+\frac{1}{3}\sum_{\substack{i=1\\(\,charged\\sleptons)}}^{6}\log\frac{m_{\tilde{l}_i}}{M_Z}\\ &+\frac{4}{3}\sum_{i=1}^{2}\log\frac{M_{C_i}}{M_Z}+\frac{1}{3}\log\frac{M_{H^+}}{M_Z}+\frac{16}{9}\log\frac{M_t}{M_Z}-7\log\frac{M_W}{M_Z}\Big).\end{aligned} \tag{11}$$

The $\overline{DR}$ values of $\alpha_i,\ (i=1,2,3)$ are converted to the corresponding $\overline{MS}$ values using the relations

$$\frac{1}{\alpha_i(M_Z)|_{\overline{MS}}} = \frac{1}{\alpha_i(M_Z)|_{\overline{DR}}}+C_i\,;\qquad \text{with}\quad C_i=\frac{C_2(G_i)}{12\pi}, \tag{12}$$

where the quadratic Casimir $C_2(G_i)=N$ for SU(N) or equals zero for U(1).

The strong coupling constant is now ready for comparison with the experimental value quoted in table 1. The electromagnetic fine structure constant may stay within the $\overline{DR}$ scheme and it is corrected by an additional factor 0.0684 ([14] and the references therein) to account for the running down to the zero momentum transfer value as extracted from Thomson scattering.

Note that $\sin^2\theta_W$ in eq.(8) represents the MSSM value, in the $\overline{DR}$ scheme, which can differ by a few *per cent* from the SM value - as found in [14]. For completeness, we also

calculate the SM value, in the $\overline{MS}$ scheme, and quote both quantities in table 8. Our SM value of $\sin^2\theta_W(M_Z)$ is obtained from the SM values of α_1 and α_2 (by a relation analogous to eq.(8)). The latter are derived from the corresponding MSSM values by applying the threshold corrections similar to (10) and (11), with the W, Z and *top* quark terms absent, since these particles are kept in the SM. These are the leading logarithmic thresholds (LLT) which make up for the exclusion in the SM of the SUSY partners and non-minimal Higgs sector.[9] A constant due to the change from the $\overline{DR}$ scheme to the $\overline{MS}$ scheme is added to $\delta\alpha_2$, according to eq.(12).

In the absence of direct observations, the SUSY sector of the MSSM is tested by all observables calculated at the loop level. Obviously, the strongest constraints come from the phenomena which originate directly in loop effects. Because of this reason ρ_{new}, as well as the process $b \to s\gamma$, were added to the list of observables. Breaking of custodial $SU(2)$ by physics beyond the SM is tested using

$$\rho_{new} = \frac{\Pi^{WW}_{new}(0)}{M_W^2} - \frac{\Pi^{ZZ}_{new}(0)}{M_Z^2}, \tag{13}$$

where $\Pi^{WW}_{new}(0)$ and $\Pi^{ZZ}_{new}(0)$ stand for the contributions of physics beyond the SM to the vector boson self-energies at zero momentum [16].

For the fermionic sector, we have at tree level $\mathbf{m}_u = Y_u \sin\beta\,\frac{v}{\sqrt{2}}$, $\mathbf{m}_d = Y_d \cos\beta\,\frac{v}{\sqrt{2}}$ and $\mathbf{m}_e = Y_e \cos\beta\,\frac{v}{\sqrt{2}}$, where $\mathbf{m}_i$ and Y_i $(i = u, d, e)$ are 3×3 mass and Yukawa matrices at M_Z. In addition, at M_Z we include the leading ($O(\tan\beta)$) one loop threshold corrections to the mass matrices [4]. The one-loop corrected fermion mass matrices are then diagonalized. The pole mass of the top quark is calculated from the diagonal running mass with the leading two loop QCD corrections included. We utilize the infrared fixed point behaviour of the top Yukawa coupling and the fact that α_s also changes only slightly between M_{top} and M_Z, and evaluate the top pole mass from the relevant couplings at the Z scale.[10] The other quark and lepton masses are run down to their corresponding mass scales as explained in the beginning of this section. M_b and M_c are evaluated using the two loop QCD corrections while the lepton pole masses are obtained with the help of the one loop QED corrections. Upon diagonalizing the one loop corrected mass matrices at M_Z, we calculate the complete

[9] Explicit forms of the LLT corrections to α_1 and α_2 are given e.g. by the equations (17) and (18) in ref.[14]. We agree with the authors of [14] that the LLT approximation cannot proceed in a consistent way at this point since the $SU(2)\times U(1)$ gauge symmetry is broken at a scale comparable to the masses of sparticles being integrated out. The difference compared to the full calculation, however, is not very significant, and for our purposes will be neglected. Thus our SM value of $\sin^2\theta_W$ contains a theoretical uncertainty of about 1%, (which is larger than the experimental uncertainty) similar to the theoretical uncertainty assigned to G_μ.

[10] A more precise evaluation would use $\alpha_s(m_t)$ and $m_t(m_t)$ to obtain the pole mass M_t. The error obtained with our approximation, using values at M_Z instead, partially cancels the one due to the non inclusion of the logarithmic corrections to the top mass, leading to a value which differs by less than 2 GeV from the actual value of M_t.

form of the CKM mixing matrix (note that the CKM matrix elements do not run below the Z scale), and then compute the theoretical value for $\hat{B}_K$ needed to fit ϵ_K[30]. The effects of SUSY box diagrams are neglected in this last calculation, while a potentially significant ($O(\tan\beta)$) one loop threshold correction to J [4] is included (automatically, since we start from the one loop corrected mass matrix $\mathbf{m}_d$) as a leading higher order effect to the SM box diagram. The SUSY box diagram corrections can be as large as 15% [32] and may affect the predictions for CP violating parameters, such as η or $\sin 2\alpha$ and $\sin 2\beta$. We discuss the sensitivity of our results to these corrections in section V.

Finally, special attention is paid to the branching ratio for $b \to s\gamma$. We calculate the partial amplitudes for this process, as well as the amplitude for $b \to s\,gluon$ (required to resum leading logarithmic corrections), using the complete quark *and squark* mixing matrices at low energies [33]. Large QCD corrections are resummed to leading order following [34]. The low scale in this evaluation is set equal to the pole mass M_b of the b quark, and the dependence of the branching ratio on this choice is neglected compared to the experimental error.

We then form a χ^2 function including the 20 low energy observables — 6 in the gauge sector (M_W, M_Z, α_{EM}, G_μ, α_s, ρ), 13 in the fermion mass sector (9 charged fermion masses, 3 quark mixing angles and $\hat{B}_K$) and the branching ratio for $b \to s\gamma$. This χ^2 function is then minimized self-consistently using Minuit by iteratively varying the GUT parameters with m_0, $M_{1/2}$, and μ fixed. The procedure involves two nested minimizations. The GUT scale parameters m_{H_d} and m_{H_u} are varied separately in the second nested minimization, for each step in the main minimization process where the rest of the free parameters are varied. Such a nested minimization is time consuming, but on the other hand it guarantees a high precision in the optimization process which is very sensitive to radiative electroweak symmetry breaking. Analytic tree level conditions for the potential minimum are used to determine v and $\tan\beta$. With these technical details we conclude the discussion on the theoretical calculation of the twenty observables given in table 1.

In addition to the 20 observables discussed above, we have to deal with the experimental lower bounds on sparticle masses. We set lower limits of 30 GeV on squark and slepton masses, expecting significant positive higher order corrections to the squared mass which would raise it above the experimental lower bound of 45 GeV. We require that the lightest neutralino (if below the LEP1 threshold) contribute to the invisible Z partial width as measured at LEP1 – $\Gamma(Z \to \text{invisibles}) = (-1.5 \pm 2.7) MeV$ [35]. We also demand that the lightest chargino be heavier than 65 GeV. Finally we require the pseudo-scalar Higgs, A, to have mass greater than 80 GeV. Note that these bounds are on the tree level running masses. In table 8 which shows predictions of the models discussed in the next sections, Higgs masses are displayed with the leading one loop corrections included.[11] As can be seen,

[11] This CP odd state A, if light, (along with the other light Higgs states) receives significant corrections to its tree level mass in the regime of large $\tan\beta$ in which we work. If the pseudoscalar mass is less than M_Z, it receives negative mass squared corrections; the same is true for the lightest CP even Higgs h^0 [36].

the 80GeV lower limit on the tree masses provides enough room for the one loop corrected Higgs masses to stay above the experimental limits. In order to take all these bounds into account we have added a large penalty to the χ^2 function whenever one of these bounds is exceeded, thus forcing the optimization procedure to stay within the experimentally allowed region in parameter space.

4 Model 4 of ADHRS

In this paper we have analyzed several models of fermion masses. We have studied model 4 of ADHRS[5]. In this model $n_y = 5$. The model is defined by the following 4 operators in the effective theory at M_G.

$$\begin{aligned} \mathcal{O}_{33} &= 16_3\ 10_1\ 16_3 \\ \mathcal{O}_{23} &= 16_2\ \frac{A_2}{\tilde{A}}\ 10_1\ \frac{A_1}{\tilde{A}}\ 16_3 \\ \mathcal{O}_{12} &= 16_1\ \left(\frac{\tilde{A}}{\mathcal{S}_M}\right)^3\ 10_1\ \left(\frac{\tilde{A}}{\mathcal{S}_M}\right)^3\ 16_2 \end{aligned} \tag{14}$$

There are six possible choices for the 22 operator; all give the same $0:1:3$ Clebsch relation between up quarks, down quarks and charged leptons responsible for the Georgi-Jarlskog relation[37].

$$\begin{aligned} \mathcal{O}_{22} = & \\ & (a) \quad 16_2\ \frac{\tilde{A}}{\mathcal{S}_M}\ 10_1 \frac{A_1}{\tilde{A}} 16_2 \\ & (b) \quad 16_2\ \frac{\mathcal{S}_G}{\tilde{A}}\ 10_1\ \frac{A_1}{\mathcal{S}_M}\ 16_2 \\ & (c) \quad 16_2\ \frac{\tilde{A}}{\mathcal{S}_M}\ 10_1\ \frac{A_1}{\mathcal{S}_M}\ 16_2 \\ & (d) \quad 16_2\ 10_1\ \frac{A_1}{\tilde{A}}\ 16_2 \\ & (e) \quad 16_2\ 10_1\ \frac{\tilde{A}\ A_1}{{\mathcal{S}_M}^2}\ 16_2 \\ & (f) \quad 16_2\ 10_1\ \frac{A_1 \mathcal{S}_G}{\tilde{A}^2}\ 16_2 \end{aligned} \tag{15}$$

A_1, A_2 and $\tilde{A}$ are adjoint scalars with vacuum expectation values [vev] in the B-L, Y or X (SU(5) invariant) directions of SO(10) and $\mathcal{S}_M$ is a singlet with vev of order M.

The resulting Yukawa matrices at M_G are given by –

$$Y_u = \begin{pmatrix} 0 & C & 0 \\ C & 0 & -\frac{1}{3}B \\ 0 & -\frac{4}{3}B & A \end{pmatrix}$$
$$Y_d = \begin{pmatrix} 0 & -27C & 0 \\ -27C & Ee^{i\phi} & \frac{1}{9}B \\ 0 & -\frac{2}{9}B & A \end{pmatrix}$$
$$Y_e = \begin{pmatrix} 0 & -27C & 0 \\ -27C & 3Ee^{i\phi} & B \\ 0 & 2B & A \end{pmatrix}.$$

where the Yukawa matrices are defined by the couplings — $H_u Q Y_u \overline{U} + H_d Q Y_d \overline{D} + H_d L Y_e \overline{E}$ and, for example, the fields $Q(\overline{U})$ are left-handed Weyl spinors transforming as a weak doublet (singlet).

The best fits give $\chi^2 \sim 13 - 14$ for 5 degrees of freedom. See figures 1a - c for contour lines of constant χ^2 in the $m_0 - M_{1/2}$ plane for different values of μ.[12] Note that the regions with lowest χ^2 contain significant (of order (4 - 9)%) one loop SUSY threshold corrections to fermion masses and mixing angles. These one loop SUSY threshold corrections scale roughly as $\frac{\mu M_{1/2}}{m_0^2}$ or $\frac{\mu A_{33}}{m_0^2}$. Hence, from figures 1a - c, we see that these corrections are necessary to improve the agreement of the model with the data.

In table 3 we give the results for the point labelled "II" in fig. 1a. All low energy observables are fit to within their 2σ bounds. However the fits for 4 observables, (V_{cb}, V_{ub}/V_{cb}, $\hat{B}_K$ and Q) lie close to the 2σ border. Note that Minuit typically tries to equalize the contribution of all the observables to χ^2. We now argue that these results are true predictions of the theory.

Consider the first three parameters. It was shown by Hall and Rasin[38] that the relation

$$\frac{V_{ub}}{V_{cb}} = \sqrt{\frac{\lambda_u}{\lambda_c}} \tag{16}$$

holds for any fermion mass texture in which the 11, 13 and 31 elements of the mass matrices are zero and perturbative diagonalization is permitted. Note λ_u, λ_c are the up and charm quark Yukawa couplings evaluated at a common renormalization scale. A typical value for the right-hand side of the equation is 0.05 which is too small for the left-hand side by more than 20%.

We now show that the fits for V_{ub}/V_{cb}, V_{cb} and $\hat{B}_K$ are correlated. Consider the formula for ϵ_K given by

$$\epsilon_K \approx \left(\frac{V_{ub}}{V_{cb}} V_{cb}^2 sin(\xi)\right) \hat{B}_K \times (\text{one loop factors}) \tag{17}$$

where the first factor is just the Jarlskog parameter, J - see eqn.(1). We see that if V_{ub}/V_{cb} is small, then V_{cb} and $\hat{B}_K$ must be increased to compensate. As a consequence, V_{cb} and $\hat{B}_K$

[12] $M_{1/2}$ and m_0 are GUT scale values, while μ is given at M_Z.

are both too large. The addition of 13 and 31 mass terms modifies relation (16) and can, in principle, accomodate larger values of V_{ub}/V_{cb} and thus lower values for V_{cb} and $\hat{B}_K$.

Now consider the ellipse parameter Q. This parameter is strongly controlled by the Georgi-Jarlskog relation[37]

$$\frac{m_s}{m_d} \approx \frac{1}{9}\frac{m_\mu}{m_e} \tag{18}$$

which is satisfied by model 4. This is an important zeroth order relation to try to satisfy. However unless there are small calculable corrections to this relation, it leads to values of $m_s/m_d \sim 25$ and thus values of Q which are too large. Note, that introducing 13 and 31 terms in the down quark and charged lepton mass matrices can also, in principle, perturb the zeroth order Georgi-Jarlskog relation.

Thus the disagreement between model 4 and the data seems significant. It is unlikely that it can be fixed with the inclusion of small threshold corrections to the Yukawa relations at M_G.[13] Before one adds new operators, however, it is worthwhile to consider the possibility that perhaps one of the experimental measurements is wrong. It is interesting to ask whether the agreement with the data can be significantly improved by removing one contribution to the χ^2 function; essentially discarding one piece of data[14]. In order to check this possibility we have artificially inflated the value of σ in the analysis for several observables (one at a time), to see if this significantly improves the fit. Our results are given in figure 2, where we also state, in the figure caption, the preferred value of the observable with the inflated error. As one can see, we find no significant improvements with this procedure.

On the other hand, we have found that we can indeed improve the results by adding one operator contributing to the 13 and 31 elements of the Yukawa matrices. We discuss this possibility in the next section. The additional terms correspond to one new effective mass operator. Of course there are many possible 13 operators. In this work we have not performed a search over all possible 13 operators. Instead we study two 13 operators which are motivated by two complete SO(10) extensions of model 4.

Finally, we should note that we have also studied the other 8 models of ADHRS. The χ^2 values for these models are significantly larger than those for model 4 discussed here.

5 Models 4(a,b,c) of LR

In this section we analyze two models derived from complete SO(10) SUSY GUTs discussed recently by Lucas and S.R.[7]. The models were constructed as simple extensions of model 4 of ADHRS. The label (a,b,c) refers to the different possible 22 operators which give identical

[13]Note, there are 2 types of threshold corrections. First, there are the higher dimension operator corrections to the 4 operators; obtained when integrating out the Froggatt-Nielsen massive intermediates. These are expected to be of order 10%. Second, there are the usual higher loop corrections.

[14]We thank M. Barnett for bringing this idea to our attention.

Clebsch relations for the 22 element of the Yukawa matrices.[15] However in the extension to a complete SUSY GUT these different operators lead to inequivalent theories. The different theories are defined by the inequivalent U(1) quantum numbers of the states. When one demands "naturalness", i.e. includes all terms in the superspace potential consistent with the symmetries of the theory one finds an additional 13 operator for models 4a and 4c given by –

$$\mathcal{O}_{13} = \tag{19}$$
$$(a) \quad 16_1 \left(\frac{\tilde{A}}{\mathcal{S}_M}\right)^3 10_1 \left(\frac{\tilde{A}A_2}{\mathcal{S}_M{}^2}\right) 16_3$$
$$(c) \quad 16_1 \left(\frac{\tilde{A}}{\mathcal{S}_M}\right)^3 10_1 \left(\frac{A_2}{\mathcal{S}_M}\right) 16_3$$

Model 4b, on the other hand, is identical to model 4 of ADHRS when states with mass greater than M_G are integrated out. The results for this model are identical to those presented in the previous section; thus we will not discuss it further. The other two models include one new effective operator at the GUT scale. The addition of this 13 operator introduces two new real parameters in the Yukawa matrices at M_G; thus we have $n_y = 7$. Models 4a and 4c differ only by the 13 operator. The resulting Yukawa matrices are given by –

$$Y_u = \begin{pmatrix} 0 & C & u_u De^{i\delta} \\ C & 0 & -\frac{1}{3}B \\ u'_u De^{i\delta} & -\frac{4}{3}B & A \end{pmatrix}$$
$$Y_d = \begin{pmatrix} 0 & -27C & u_d De^{i\delta} \\ -27C & Ee^{i\phi} & \frac{1}{9}B \\ u'_d De^{i\delta} & -\frac{2}{9}B & A \end{pmatrix}$$
$$Y_e = \begin{pmatrix} 0 & -27C & u_e De^{i\delta} \\ -27C & 3Ee^{i\phi} & B \\ u'_e De^{i\delta} & 2B & A \end{pmatrix}$$

where the new Clebsches for models 4(a,c) are given in table 2.

We find that model 4a gives a best fit $\chi^2 \sim 4$ for 3 dof, while model 4c gives $\chi^2 \leq 1$ for 3 dof. For model 4c, our best fit with $\chi^2 = 0.168$ is found for $\mu = 160GeV, M_{1/2} = 400GeV, m_0 = 2900GeV$. Our results are presented in figures [3(a - c)] for model 4a and figures [4(a - c)] for model 4c.

In order to understand why the 13 operator resolves the problems discussed in the previous section, consider the approximate formulas (valid to 10% and particular to model 4c)

[15]Note, models d, e and f have the second family 16_2 coupled directly to 10_1 and a heavy 16. If this coupling is as large as the third generation Yukawa coupling, then we would obtain excessively large flavor changing neutral current processes, such as $\mu \to e\gamma$. Thus these models were not considered in [7].

for V_{ub}/V_{cb}, V_{cb}, λ_s, λ_d, λ_μ, λ_e where the latter are the diagonalized Yukawa eigenvalues and all are evaluated at the GUT scale. We have

$$\begin{aligned} V_{ub}/V_{cb} &= \frac{9\,C\,A}{4\,B^2} \\ V_{cb} &= \frac{4\,B}{9\,A} \\ \lambda_s &= E \\ \lambda_d &= \frac{729\,C^2}{E}\left(1-\frac{31}{243}\frac{B\,D}{C\,A}e^{-i\,\delta}\right) \\ \lambda_\mu &= 3\,E \\ \lambda_e &= \frac{243\,C^2}{E}\left(1-\frac{109}{27}\frac{B\,D}{C\,A}e^{-i\,\delta}\right) \end{aligned} \tag{20}$$

(21)

Recall, the contribution of the 13 operator is proportional to D. Consider first the electron and down quark Yukawa couplings. The electron gets a significant correction from the 13 operator whereas the correction to the down quark is much smaller. When one adds the 13 operator to a model which is already fit to the lepton masses, one must readjust the parameters. In order to keep the electron mass fixed, one needs to increase the parameter C [note, in the fits $\delta \sim 2\pi$]; the parameter E is kept fixed in order not to change the muon mass. As a consequence the ratio V_{ub}/V_{cb} increases, which allows for smaller values of $\hat{B}_K$. In addition we see that the Georgi - Jarlskog relation is now given by

$$\frac{m_s}{m_d} \approx \frac{1}{9}\left(\frac{1-\frac{109}{27}\frac{B\,D}{C\,A}e^{-i\,\delta}}{1-\frac{31}{243}\frac{B\,D}{C\,A}e^{-i\,\delta}}\right)\frac{m_\mu}{m_e}$$

As a consequence, the ratio 1/9 is further decreased; hence Q is reduced. Thus one new operator is able to resolve four problems.

Let us now discuss our results for model 4c. We find the preferred region of SUSY parameter space with a fixed value of $\mu = 80$GeV corresponds to $M_{1/2} > 220$GeV and $m_0 > 300$GeV. The lower bound on m_0 depends slowly on $M_{1/2}$ while the lower bound on $M_{1/2}$ appears to be independent of m_0. These bounds are rather distinct (the χ^2 value rises steeply when getting closer to these values) since they result from the lower experimental limits on sparticle masses. No observable from our list in table 1 places a decisive constraint which would exclude a portion of the $(m_0, M_{1/2})$ parameter space at fixed $\mu = 80$GeV. In other words, for this value of μ everything in the $(m_0, M_{1/2})$ plane that has not been excluded by direct experimental searches, is allowed (provided the other parameters are subject to the optimization procedure).

As μ increases (see figs. 4b and 4c for $\mu = 160,\ 240$ GeV, resp.) the lower bound on $M_{1/2}$ goes down since it is determined by the LEP limits on the masses of the lightest chargino and neutralino. The latter become proportional to, but less than, $M_{1/2}$ in the limit of large μ. In addition, as μ increases the χ^2 profile in the m_0 direction starts to change

more smoothly, and the contour lines of constant χ^2 shift more towards the higher values of m_0. This is explained by the fact that the constraints placed by the observables which receive one loop corrections enhanced by tanβ start to be significant. (Especially the b quark mass correction and subsequently the correction to $M_b - M_c$.) Since these one loop SUSY threshold corrections scale roughly as $\mu\, M_{1/2}/m_0^2$ or $\mu\, A_{33}/m_0^2$ we see that with increasing μ a larger suppression by m_0 is required to keep the potentially large corrections under control. The effect clearly shows up in figures 4a,b,c combined.

Our results show that the SUSY sector can make its presence visible in the analysis of the SM fermion mass parameters, especially those suppressed by tanβ at tree level, through the low energy threshold corrections. For $\chi^2 \sim 1$ the latter are up to 9%. Two notes are in order at this point: First, note that these corrections have the potential to be as large as 30-70% [16][3]. It would be interesting if a window in parameter space with such large SUSY contributions was favored. However, our numerical optimization never disclosed such a region. Second, it is interesting to note that the best fit is found in the region of very large m_0, where the effect of the SUSY threshold corrections to fermion masses and mixings is, in fact, minimized. As a result, in this region, with $\chi^2 < 1$ and the SUSY corrections to fermion masses negligible, the effective number of degrees of freedom is actually larger than 3, since there are 7 parameters in the Yukawa matrices determining the 13 low energy observables in the fermion mass sector. *This means that the Yukawa sector of the selected model does actually a much better job than appears at first glance.*

For the opposite sign of μ there is a significant restriction from the process $b \to s\gamma$. As, has been noticed by many authors, the SM amplitude with the W in the loop is sufficiently big to explain the measured branching ratio. In the large tanβ regime of the MSSM however, there are substantial partial amplitudes due to the charged Higgs and chargino loops. The charged Higgs amplitude is always of the same sign as the SM amplitude, while the sign of the chargino amplitude depends on the sign of μA_t. In order to get an agreement with the measured rate, the chargino amplitude, especially with large tanβ, has to enter with the opposite sign, and as a consequence a specific sign of μA_t is preferred. Due to the boundary conditions at the GUT scale which are used throughout this paper we always run into the region at the Z scale where $A_t < 0$, and as a result the sign of μ is fixed. ($\mu > 0$, in our convention.) With the bad sign of μ, the best χ^2 values are about 30.[17] For this reason we do not quote results or figures for $\mu < 0$. Interestingly enough, even if we exclude the branching ratio for $b \to s\gamma$ from the list of observables and repeat the optimization procedure for $\mu < 0$, the conspiracy between the one loop corrections proportional to μ (see the two

[16] Clearly, such large corrections would not violate perturbativity, since the main reason for them being large would be that the corresponding tree level values happen to be tanβ suppressed. That means that the higher order corrections would be well under control as for any other quantity not suppressed at tree level.

[17] Obviously, if superpartners are *very* heavy, the SUSY spectrum decouples and the above statement is incorrect. However, for large tanβ, "*very* heavy" in this case means deep in the TeV region which we don't consider in our analysis.

previous paragraphs) does not work very well and significantly worse χ^2 values are obtained than in the case $\mu > 0$.

Finally note that $|\mu|$ less than about 65GeV is excluded since there would inevitably be a light higgsino-like neutralino and chargino; already ruled out by experiment. Moreover, the large values of m_0 selected by our fit, imply a suppression of the supersymmetric corrections to the anomalous magnetic moment of the muon, which could otherwise lead to very strong constraints on the allowed parameter space in the large $\tan\beta$ region [43].

In tables 4 - 7 we give the values of the initial parameters which minimize χ^2 for fixed particular values of $\mu,\ m_0,\ M_{1/2}$ labelled as points I-III marked in figures 4a-c. For each low energy observable we quote its computed value, the partial contribution to χ^2 and the relative magnitude of the SUSY threshold corrections [in %]. We also include in tables 8 and 9 values for the SUSY and Higgs spectra, the unitarity triangle parameters ρ, η together with the corresponding angles $\alpha,\ \beta$ and γ, measurable in neutral B decays, and the predicted ratio for m_u/m_d.

Note that the values for $\alpha,\ \beta$ and γ do not significantly change across different points in the SUSY parameter space. This fact is explicitly evident from figure 5. Each "x"-symbol in this figure stands for a point anywhere in the SUSY parameter space with the minimum of χ^2 less than 3, with 3 degrees of freedom present both in model 4c and model 4a. Note that, under such a restriction in model 4a, only the corner in the SUSY parameter space with very large m_0 and $M_{1/2}$ contributes to figure 5b. Nevertheless, these two models give similar, narrowly spread predictions for sin2α and sin2β , grouped around the values 0.95 and 0.52, respectively, while a much larger region is allowed for these two observables as a result of a general Standard Model analysis [44].

We have also checked the sensitivity of our results, for point I in fig. 4a, to a potential 10% positive enhancement of ϵ_K. We have found that the total χ^2 stays the same to within a few per cent and that our predictions for sin2α (sin2β) change from 0.953 (0.513) to 0.957 (0.527). Indeed, over a large range of points, we checked that the predictions for sin2α (sin2β) change by less than 1% (3%). Thus our results, for model 4c, are not very sensitive to SUSY box corrections to ϵ_K. On the other hand, for point II (fig. 3a) in model 4a, we find that a 10% positive enhancement of ϵ_K significantly improves the agreement with experiment; χ^2 changes from 6.99 to 4.57. This is because in this case, $\hat{B}_K$ was a significant constraint on the model.

It is an interesting feature of most of the points in the SUSY parameter space that the best fits favor a rather large negative GUT threshold correction ϵ_3 (eqn. 4). In figure 6a the sensitivity of the best fits to different lower bounds on ϵ_3 is displayed for values of μ and $M_{1/2}$ fixed and m_0 varied. In addition table 10 shows how the selected GUT scale parameters $\alpha_G,\ M_G$ and A (the 33 element in the Yukawa matrices) vary in the best fits at m_0=700GeV (point II), in order to compensate for changes in the lower bound on ϵ_3. Our study shows that even small positive GUT threshold corrections 1-2% to α_s are plausible in model 4c. As one can see in table 10, this would require a rather low value of the GUT scale, below 1×10^{16}GeV, and lower α_G. As a result, the best fit value of $\alpha_s(M_Z) \sim 0.116$ is getting closer

to its central value 0.118, while G_μ is getting worse. On the other hand, the A parameter of the Yukawa matrices is quite insensitive to the change in ϵ_3 and to the induced changes in α_G and M_G, and so are the masses of the heaviest generation.

We note that our results in this regard differ from those of a recent paper by Pierce et al.[45] in which a general MSSM analysis is performed. We believe that a significant part of the difference results from our assumed theoretical uncertainties in the electroweak observables. Recall, in our analysis we have assumed an overall 0.5% theoretical uncertainty (σ) for M_Z, M_W, and α_{EM} and a 1% uncertainty for G_μ. As commented previously, we believe these uncertainties correctly account for the theoretical errors introduced by neglecting higher orders in perturbation theory and by the numerical analysis. However for comparison, we have changed the theoretical uncertainties for M_Z, α_{EM}, and G_μ to 0.1% and for M_W to the experimental value of 130 MeV; the new results, for model 4c, are displayed in figure 6b and table 11. In table 11 we see that in this case α_s varies significantly with changes in ϵ_3. Moreover, as ϵ_3 increases the quality of the fit quickly deteriorates. This is seen graphically in figure 6b. We find, for point II in model 4c with ϵ_3 = -3% (-2%), χ^2 = 7.49 (13.97) with the dominant contributions to χ^2 coming from M_Z – 2.11 (3.67), G_μ – 0.89 (1.81), α_{EM} – 0.74 (1.46) and $m_b(M_b)$ – 2.05 (3.69). Thus the theoretical uncertainties for the precisely measured electroweak parameters allow for quite a bit of flexibility in the values of ϵ_3 and $\alpha_s(M_Z)$.

Since we have focused on fermion masses we have not discussed the Higgs sector of particular models in great detail in this work. However, in figure 7 we show the sensitivity of the best fits to the assumed lower bound of the pseudoscalar mass, at fixed values of μ=80GeV and $M_{1/2}$=240GeV in model 4c. As one can see, requiring a heavier pseudoscalar (A) forces the model into the region of larger m_0 and thus heavier squarks and sleptons. Or in other words, in order to have light squarks and sleptons, one necessarily also has a light A.

To understand these properties, it is instructive to analyze the renormalization group evolution of the mass parameters. For a top quark mass $M_t \simeq 175$ GeV, the low energy soft supersymmetry breaking mass parameters are approximately given by [23],

$$\begin{aligned}
m_{H_u}^2 &\simeq \frac{2}{3}\left(m_{H_u}^2(0) - m_0^2\right) - 2.5 M_{1/2}^2, \\
m_{H_d}^2 &\simeq \frac{2}{3}\left(m_{H_d}^2(0) - m_0^2\right) - 2.3 M_{1/2}^2 - \frac{0.2}{3}\left(2\, m_0^2 + m_{H_d}^2(0)\right), \\
m_Q^2 &\simeq \frac{5\, m_0^2}{9} - \frac{m_{H_u}^2(0) + m_{H_d}^2(0)}{9} + 5 M_{1/2}^2, \\
m_D^2 &\simeq \frac{5\, m_0^2}{9} - \frac{2\, m_{H_d}^2(0)}{9} + 5 M_{1/2}^2,
\end{aligned} \tag{22}$$

where m_Q and m_D are the left and right handed sbottom mass parameters, and we have ignored the A_0 contribution, as well as the small $m_{H_u}(m_{H_d})$ effect on the running of $m_{H_d}(m_{H_u})$. Moreover, in the large $\tan\beta$ regime there is a simple relation between the Higgs mass parameters and the pseudoscalar Higgs mass, namely [24],

$$m_A^2 \simeq m_{H_d}^2 - m_{H_u}^2 - M_Z^2. \tag{23}$$

Using the fact that $m_{H_u}^2 \simeq -M_Z^2/2 - \mu^2$, we obtain,

$$m_{H_u}^2(0) - m_0^2 \simeq 4M_{1/2}^2 - \frac{3}{2}\left(\mu^2 + \frac{M_Z^2}{2}\right). \tag{24}$$

Since the best fit is obtained for moderate values of the one-loop down quark mass corrections, low values of the μ parameter $\mu^2 \ll m_0^2$ are preferred. For $M_{1/2} > \mu \simeq \mathcal{O}(M_Z)$, an approximate relation between $m_{H_u}(0)$ and m_0 is obtained as a function of the gaugino mass parameter $M_{1/2}$. Moreover,

$$0.9\, m_{H_d}^2(0) - m_{H_u}^2(0) \simeq 0.1\left(2\, m_0^2 - 3\, M_{1/2}^2\right) + \frac{3}{2}(m_A^2 + M_Z^2). \tag{25}$$

From the above equations, the qualitative behaviour of our solutions may be understood. For instance, for $m_0 \simeq 3M_{1/2}$, as is the case at point II on fig. 4a (see table V), and $M_{1/2} > \mu, M_Z$, from Eq. (24) we get that $m_{H_u}(0) \simeq 1.2\ m_0$. Moreover from Eq. (25), we obtain that $m_{H_d}(0)$ may vary from values of order $1.4\ m_0$, for low values of m_A, up to values of order $2\ m_0$ for larger values of m_A, without inducing a problem in the sbottom sector. Larger values of $m_{H_d}(0)$, however, induce lower values of the sbottom mass parameters, implying unwanted large values for the gluino-induced bottom mass corrections. Therefore, the best fit is obtained for values of the CP-odd Higgs mass close to its experimental bound, or, equivalently, for values of $m_{H_d}(0)$ of the order of $1.4\ m_0$. Larger (smaller) values of $m_0/M_{1/2}$ imply smaller (larger) values of $m_{H_{u,d}}(0)/m_0$, as is clearly seen from Eqs. (24), (25) (see Tables III-VII).

The relation between the CP-odd mass and m_0 may also be understood from the above equations. For large values of the CP-odd mass, and $m_0 > M_{1/2}$, $m_{H_d}^2(0)$ must be significantly larger than $m_{H_u}^2(0)$. For these large values of $m_{H_d}^2(0)$, large values of m_0^2 are required in order to avoid a very low value of the sbottom mass. The results displayed in fig. 7 are just a reflection of this fact.

To conclude this section let's discuss how the performance of models 4a-c changes if recent lattice results on the low value of the strange quark mass prove to be correct [25]. With $m_s(1GeV) = (120 \pm 25)MeV$ replacing the value $(180 \pm 50)MeV$ of table 1, the χ^2 value of model 4c at point II changes from 0.731/3dof to a significantly worse value of 5.44/3dof. More than a half of it comes from the m_s value itself, 163.4MeV at the best fit, indicating that model 4c cannot get to such low values of the strange mass as reported by the lattice groups, even with the help of the fifth effective operator. The rest of the χ^2 value is being shared by a low value for $\alpha_s(M_Z)$, a high V_{cb} and $\hat{B}_K$, and low V_{ub}/V_{cb}, contributing by less than 0.8 to the total χ^2 each. We checked that this behaviour of model 4c is typical for different points as well, and that the best fit values of the strange quark mass $m_s < 160$MeV never occurs. Model 4a, on the contrary, favors values of $m_s(1GeV)$ less than 180MeV. However, decreasing m_s cannot cure the problems of this model: high values of $\hat{B}_K$ and V_{cb}, and a low value for V_{ub}/V_{cb}. At the same point II, these observables contribute 2.85, 0.75 and 1.76, respectively, to χ^2 which totals 6.82 despite values of m_s as low as 136.5MeV. This

represents only a marginal improvement to the χ^2 value of 6.99 at the same point with the original larger experimental value of the s-quark mass. Finally, the performance of model 4 gets slightly worse with the low value of m_s: total χ^2 changes from 14.01 to 16.16 as m_s goes from 163MeV down to 156MeV in the best fits at point II.

6 Discussion and Conclusions

The results of our analysis, as well as the whole project presented here, may be understood from two different perspectives.

The emphasis of this paper is to reanalyze the fermion mass sector in the context of the minimal SO(10) SUSY GUT in order to gain insight into the underlying flavor physics. From this perspective, we analyzed the best working model of ADHRS with four effective operators in the Yukawa sector at the GUT scale. The best fit allows us to assign a confidence level of about 3-4% to this model. Next, we found that the addition of a new operator, giving rise to the 13 (and 31) entries in the Yukawa matrices, may improve the performance of the model. Substantial improvement however, is not automatic, as has been evidenced with model 4a that has a confidence level $< 50\%$ for the best fits in the corner of SUSY parameter space with very large m_0 and $M_{1/2}$, and large μ. On the other hand, we showed that model 4c provides an excellent fit to all 20 low energy observables, with confidence level better than 68% in a large region of the allowed SUSY parameter space. We have not performed a complete search over all possible 13 operators. Model 4c was picked as a candidate model suggested by a recent formulation of a complete SO(10) SUSY GUT[7]. Whether or not this particular model is close to the path nature has chosen remains to be seen. One important test will be via the CP violating decays of the B. We predict a value for $\sin 2\alpha$ which is insensitive to the SUSY breaking parameters (see figure 5 and tables 8 and 9), whereas in the SM the value of $\sin 2\alpha$ is unrestricted[44]. Another important test will come from nucleon decay rates which is discussed in a recent paper[46].

As a separate matter, we considered the sensitivity of our results to different lower bounds for ϵ_3. For the assumed theoretical uncertainties, as given in table 1, our analysis of model 4c indicates that the best fits favor a negative GUT threshold correction to α_s of the order -(4-5)%. We have checked for the whole m_0 - $M_{1/2}$ plane at fixed $\mu = 80GeV$ that a correction of -3% instead of -(4-5)% can easily be accomodated and gives basically the same best values of χ^2 as obtained in the unrestricted analysis. In this case, for $\epsilon_3 = -3\%$, the contour lines of figure 4a move almost uniformly towards higher values of m_0 by about 50 GeV. Note that the study of the complete SO(10) model[7] giving rise to the effective operators of model 4c shows that such negative corrections to $\alpha_s(M_G)$ can easily be obtained without any fine tuning. To understand how sensitive our results might be to this threshold correction we studied a narrower region in the parameter space, determined by fixed $M_{1/2}$=240GeV at the previously fixed μ=80GeV (see figure 6a and table 10). It turns out that $\epsilon_3 > 0$ remains a possibility, at the expense of lower GUT scale and α_G, resulting in a worse agreement with

the low energy value of G_μ. Fermion masses are not very sensitive to these variations. In addition, from table 10 it is clear that as ϵ_3 increases, so does $\alpha_s(M_Z)$. These results are however strongly dependent on the magnitude of our assumed theoretical uncertainties as discussed in the previous section and shown in figure 6b and table 11.

Note that model 4c is also flexible enough to accomodate recent analyses of the R_b anomally and low values for $\alpha_s(M_Z)$ [47, 48]. For the Higgs sector of the MSSM, the best fits at a number of points (e.g. also at the sample points I - III; see tables 8 and 9) end up with low values of the pseudoscalar Higgs mass m_A. This preference is not strong though, as can be inferred from figure 7 where we show how the quality of the fits change with the increasing lower bound on m_A. However, the low value of m_A, such as at point III2 for instance, leaves the door open for a natural explanation of the 1-2σ increase in the partial width $Z \to b\bar{b}$, without ever asking for it in the course of our analysis. At the same time, as can be argued on general grounds, one of the CP even Higgs states is always almost degenerate with the pseudoscalar state. For $m_A < M_Z$ it is the lighter h^0 state, while for $m_A > M_Z$ it is the heavy Higgs state H^0. In the latter case, the h^0 mass equals $M_Z \cos^2 2\beta$ + *rad. corrections* where the radiative corrections are rather substantial in our case. Thus our study indicates that there are no additional constraints on a light CP even Higgs state between the experimental limit of about 55GeV (for $\tan\beta \simeq 60$) and the upper MSSM limit of about 130GeV.

Another interesting feature of the best fits is the tendency towards lower values of $\alpha_s(M_Z) \sim 0.115$. As with low m_A, it just happens to be in agreement with a potentially significant positive pseudoscalar contribution to R_b. The origin of rather low α_s in the best fits can be traced to the optimization efforts to suppress the gluino correction to an already large enough value for $m_b(M_Z)$. This correction has to be positive, since its sign is correlated with the sign of the chargino-stop partial amplitude to the process $b \to s\gamma$ [24], and the latter is fixed in the large tanβ regime, as described in the previous section. At the same time lower values of $\alpha_s(M_Z)$ are welcome in order to suppress the QCD logarithmic corrections to $b \to s\gamma$. Here the point is that with tanβ large the chargino-stop loop tends to be too large, most of the times outweighing by too much the W and H^+ loops which contribute with the opposite sign. Thus the optimization favors lower $\alpha_s(M_Z)$ as the way to make up for a rather large net $b \to s\gamma$ amplitude by minimizing the enhancement from the renormalization to the M_b scale.

Our analysis can also be viewed from a different perspective. Let us neglect for a moment the underlying GUT physics and the origin of the Yukawa matrices at the GUT scale and view this analysis simply as an MSSM global fit in the large $\tan\beta$ regime. (See also [48].) ¿From this new perspective a special feature of our approach is that we run complete sets of fermion and sfermion mass matrices down to the Z scale, instead of just the leading 33 elements. We now try to draw some general conclusions coming from such an analysis.

Our results suggest that there is no narrow, strongly preferred region in the SUSY $(m_0, M_{1/2})$ parameter plane for low values of the μ parameter $\mu(M_Z) \sim 80GeV$. Hence, at present one cannot make strong conclusions in the large tanβ regime about the masses of squarks, sleptons and gluinos, which leaves open various channels for Tevatron and LEPII

experiments.

In addition, a definite statement can be made about the sign of μ following from the structure of the partial amplitudes to the process $b \to s\gamma$, as already explained in more detail in the previous section. In the conventions we use μ has to be positive. Note, this conclusion, however, depends on the assumption of universal squark and slepton masses and universal A parameter at M_G which constrains the sign of A_t at M_Z.

Finally, by keeping the complete 3×3 mass matrices for both fermions and sfermions one can study flavor dependent processes in a theory which fits the low energy data; for example, in rare B and K decays, $B - \bar{B}$ mixing, lepton flavor violating processes or even $Z \to b\bar{b}$.

In summary, we performed a detailed global analysis of independent SM parameters (plus the extra low energy data constraining the SUSY sector) in several models based on SO(10) SUSY GUTs. At the present time, when direct evidence for physics beyond the Standard Model evades experimental observations, this kind of analysis serves as the best test of new physics and actually starts to compete with SM electroweak precision tests. Our ultimate goal is to identify a set of effective theories, defined at a scale M (M = M_{Planck}, M_{string} or M_{GUT}) which accurately fit the low energy data and thus determine the boundary conditions at the scale M for some more fundamental theory valid above M. We have shown that this set is non-trivial; model 4c is one element of the set. More elements of the set need to be found in order to determine (a) whether they can be distinguished by purely low energy measurements, or (b) whether one or more elements can be constructed as the low energy limit of a string.

Finally, some theoretical uncertainties in the present analysis can and should be removed in the future. By including the SUSY box contributions to G_μ we can remove the additional 1/2% uncertainty included in the evaluation of χ^2 for this quantity. In addition, the SUSY box corrections to ϵ_K can be as large as 15%[32]. These should be included in order to remove the uncertainties in the predictions for CP violating parameters; although these uncertainties do not appear to be significant at the representative points studied in model 4c.

Acknowledgments

This research was supported in part by the U.S. Department of Energy contract DE-ER-01545-681. T.B. would like to thank Piotr Chankowski for many useful discussions and Steve Martin for clarifications.

References

[1] S. Dimopoulos, S. Raby and F. Wilczek, *Phys. Rev.* **D24**, 1681 (1981); S. Dimopoulos and H. Georgi, *Nucl. Phys.***B 193**, 150 (1981); L. Ibanez and G.G. Ross, *Phys. Lett.*

105B, 439 (1981); M. B. Einhorn and D. R. T. Jones, *Nucl. Phys.* **B196**, 475 (1982); W. J. Marciano and G. Senjanovic, *Phys. Rev.* **D 25**, 3092 (1982). For recent analyses, see P. Langacker and N. Polonsky, *Phys. Rev.***D47**, 4028 (1993); ibid., **D49**, 1454 (1994); M. Carena, S. Pokorski, C.E.M. Wagner, *Nucl. Phys.***B406**, 59 (1993).

[2] H. Georgi, Particles and Fields, Proceedings of the APS Div. of Particles and Fields, ed C. Carlson; H. Fritzsch and P. Minkowski, *Ann. Phys.* **93**, 193 (1975).

[3] L.J. Hall, R. Rattazzi and U. Sarid, *Phys. Rev.* **D50**, 7048 (1994); M. Carena, M. Olechowski, S. Pokorski and C. Wagner, *Nucl.Phys.***B426**, 269 (1994); R. Hempfling, *Phys. Rev.* **D49**, 6168 (1994).

[4] T. Blažek, S. Raby and S. Pokorski, *Phys. Rev.* **D52**, 4151 (1995).

[5] G. Anderson, S. Dimopoulos, L.J. Hall, S. Raby and G. Starkman, *Phys. Rev.***D49**, 3660 (1994).

[6] M. Carena, S. Dimopoulos, S. Raby and C.E.M. Wagner, *Phys. Rev.***D52** 4133 (1995).

[7] V. Lucas and S. Raby, *Phys. Rev.***D54**, 2261 (1996).

[8] D. Kaplan and A. Manohar, *Phys. Rev. Lett.* **56**, 2004 (1986); H. Leutwyler, *Nucl. Phys.***B337**, 108 (1990).

[9] C. Jarlskog, *Phys. Rev. Lett.* **55**, 1039 (1985).

[10] M.Schmelling, "α_s (determination and implications)", plenary talk at the 28th International Conference on High Energy Physics, Warsaw, Poland, July 25 - 31, 1996. To be published in the conference proceedings.
The same value is also quoted by I.Hinchliffe (Particle Data Group) in the "Review of Particle Physics", *Phys. Rev.* **D54**, 1 (1996), page 77.

[11] B.R. Webber, "QCD AND JET PHYSICS," plenary talk at 27th Int Conf on HEP, Glasgow, July 1994.

[12] P.Burrows, "Review of α_s Measurements", invited talk at the 3rd International Symposium on Radiative Corrections, Cracow, Poland, August 1 - 5, 1996. To be published in the conference proceedings.

[13] W.J.Marciano and A.Sirlin, *Phys. Rev. Lett.***61**, 1815 (1988).

[14] P. Chankowski, Z. Pluciennik and S. Pokorski, *Nucl. Phys.***B439**, 23 (1995).

[15] R. Gupta, D. Daniel, G.W. Kilcup, A. Patel and S.R. Sharpe, *Phys. Rev.* **D47**, 5113 (1993); G. Kilcup, *Phys. Rev. Lett.* **71**, 1677 (1993); S. Sharpe, Nucl. Phys. B (Proc. Suppl.) **34**, 403 (1994).

The same mean value and standard deviation for B_K were given in a recent review article: U.Nierste,"Phenomenology of ϵ_K in the Top Era", invited talk at the workshop on K physics, Orsay, France, May 30 - June 4, 1996 (LANL hep-ph/9609310).

[16] P.Langacker, "Tests and Status of the Standard Model", invited talk at SUSY'96 Conference in College Park, MD, May 29 - June 1, 1996 (to be published in the conference proceedings); and the update after the summer'96 conferences (private communication).

[17] A.Manohar (Particle Data Group) in the "Review of Particle Physics", *Phys. Rev.* **D54**, 1 (1996), page 303; P. Ball, M. Beneke, V. M. Braun, *Phys. Rev.***D52**, 3929 (1995).

[18] P. Ball, M. Beneke and V.M. Braun, CERN preprint CERN-TH/95-26 (hep-ph/9502300) (1995).

[19] J.F. Donoghue, B. Holstein and D. Wyler, *Phys. Rev.* **D47**, 2089 (1993); J. Bijnens, *Phys. Lett.* **B306**, 343 (1993); A. Duncan, E. Eichten and H. Thacker, *Phys. Rev. Lett.* **76**, 3894 (1996). Summarized in H. Leutwyler, *Phys. Lett.* **B378**, 313 (1996).

[20] J.F.Donoghue, "Light Quark Masses and Mixing Angles", in the proceedings "The Building Blocks of Creation" of TASI'93, ed. S.Raby and T.Walker, World Scientific, 1994.

[21] H. Leutwyler, CERN preprint CERN-TH/96-44 (hep-ph/9602366) (1996).

[22] (Particle Data Group) in the "Review of Particle Physics", *Phys. Rev.* **D54**, 1 (1996).

[23] See, for example, D. Mattaliotakis and H.P. Nilles, *Nucl. Phys.***B435**, 115 (1995); M. Olechowski and S. Pokorski, *Phys. Lett.* **B344**, 201 (1995).

[24] Work by M.Carena et al. in ref.[3]

[25] R. Gupta and T. Bhattacharya, Los Alamos preprint LA-UR-96-1840, May 1996 (LANL hep-lat/9605039); B.J. Gough, G.M. Hockney, A.X. El-Khadra, A.S. Kronfeld, P.B. Mackenzie, B.P. Mertens, T. Onogi and J.N. Simone, Fermilab preprint FERMILAB-PUB-96-283, October 1996 (LANL hep-ph/9610223).

[26] S.P. Martin and M.T. Vaughn, *Phys. Rev.* **D50**, 2282 (1994).

[27] H. Arason, D.J. Castaño, B. Kesthelyi, S. Mikaelian, E.J. Piard, P. Ramond and B.D. Wright, *Phys. Rev.* **D46**, 3945 (1992); V. Barger, M.S. Berger, and P. Ohmann, *Phys. Rev.* **D47**, 1093 (1993).

[28] W. Hollik, in "Precision Tests of the Standard Electroweak Model", ed. P. Langacker, World Scientific, 1995.

[29] G. Degrassi, S. Fanchiotti and A. Sirlin, *Nucl. Phys.***B351**, 49 (1991).

[30] T.Inami and C.S.Lim, *Prog. Theor. Phys.* **65**, 297 (1981); U.Nierste and S.Herrlich, "Phenomenology of ϵ_K Beyond Leading Logarithms", talk presented at the EPS-HEP 95 conference, Brussels, Jul.27-Aug.2 1995 (LANL hep-ph/9510383) .

[31] M. Dugan, B. Grinstein and L.J. Hall, *Nucl. Phys.***B255**, 413 (1985).

[32] T. Goto, T. Nihei and Y. Okada, *Phys. Rev.* **D53**, 5233 (1996).

[33] S.Bertolini, F.Borzumati, A.Masiero and G.Ridolfi, *Nucl. Phys.* **B353**, 591 (1991).

[34] B.Grinstein, R.Springer and M.B.Wise, *Phys. Lett.* **B202**, 138 (1988) and *Nucl. Phys.* **B339**, 269 (1990).

[35] P.Renton, Rapporteur talk at the International Symposium on Lepton and Photon Interactions at High Energies, Beijing, August 1995, Oxford preprint OUNP-95-20 (1995).

[36] H.E. Haber and R. Hempfling, *Phys. Rev.* **D48** 4280 (1993); M.Carena, J.R.Espinoza, M.Quiros and C.E.M.Wagner, *Phys. Lett.* **B355**, 209 (1995); D.M.Pierce, J.Bagger, K.Matchev and R.Zhang, SLAC preprint SLAC-PUB-7180, June 1996, (LANL hep-ph/9606211) .

[37] H. Georgi and C. Jarlskog, *Phys. Lett.* **B86**, 297 (1979).

[38] L.J. Hall and A. Rasin, *Phys. Lett.* **B315**, 164 (1993).

[39] S. Weinberg, *Phys. Rev.* **D26**, 287 (1982); N. Sakai and T. Yanagida, *Nucl. Phys.* **B197**, 533 (1982).

[40] S. Dimopoulos, S. Raby and F. Wilczek, *Phys. Lett.***112B**, 133 (1982); J. Ellis, D.V. Nanopoulos and S. Rudaz, *Nucl. Phys.***B202**, 43 (1982). For recent analyses, see R. Arnowitt and P. Nath, *Phys. Rev.***D49**, 1479 (1994); J. Hisano, H. Murayama, and T. Yanagida, *Nucl. Phys.***B402**, 46 (1993); P. Langacker, "Proton Decay," (LANL hep-ph/9210238) talk given at The Benjamin Franklin Symposium in Celebration of the Discovery of the Neutrino, Philadelphia, PA, 29 Apr - 1 May (1992).

[41] S. Weinberg, *Phys. Lett.* **91B**, 51 (1980); L.J. Hall, *Nucl. Phys.* **B178**, 75 (1981).

[42] See, S. Dimopoulos and H. Georgi, [1]; L.J. Hall, V. A. Kostelecky, and S. Raby, *Nucl. Phys.* **B267**, 415 (1986); H.Georgi, *Phys. Lett.* **B169**, 231 (1986) and S. Dimopoulos and A. Pomarol, *Phys. Lett.* **B353**, 222 (1995).

[43] J. Lopez, D.V. Nanopoulos, and X. Wang, *Phys. Rev.* **D49** 366 (1991); U. Chattopadhyay and P. Nath, *Phys. Rev.* **D53** 1648 (1996); T. Moroi, *Phys. Rev.* **D53** 6565 (1996); M. Carena, G.F. Giudice and C.E.M. Wagner, CERN preprint CERN-TH/96-271 (hep-ph/9610233).

Table 1: Experimental observables

Observable	Central value	σ
M_Z	91.186	0.46
M_W	80.356	0.40
G_μ	$1.166 \cdot 10^{-5}$	$1.2 \cdot 10^{-7}$
α_{EM}^{-1}	137.04	0.69
$\alpha_s(M_Z)$	0.118	0.005
ρ_{new}	$-0.6 \cdot 10^{-3}$	$2.6 \cdot 10^{-3}$
M_t	175.0	6.0
$m_b(M_b)$	4.26	0.11
$M_b - M_c$	3.4	0.2
m_s	180	50
m_d/m_s	0.05	0.015
Q^{-2}	0.00203	0.00020
M_τ	1.777	0.0089
M_μ	105.66	0.53
M_e	0.5110	0.0026
V_{us}	0.2205	0.0026
V_{cb}	0.0392	0.003
V_{ub}/V_{cb}	0.08	0.02
$\hat{B}_K$	0.8	0.1
$B(b \to s\gamma)$	$2.32 \cdot 10^{-4}$	$0.92 \cdot 10^{-4}$

[44] A. Ali and D. London, DESY preprint DESY 96-140 (hep-ph/9607392) (1996).

[45] D.M. Pierce, J.A. Bagger, K. Matchev and R. Zhang, SLAC preprint SLAC-PUB-7180 (hep-ph/9606211) (1996).

[46] V. Lucas and S. Raby, OSU preprint OHSTPY-HEP-T-96-030 (hep-ph/9610293) (1996).

[47] A. Blondel and C. Verzegnassi, *Phys. Lett.***B311** 346 (1993); G.L. Kane, R.G. Stuart and J.D. Wells, *Phys. Lett.***B354** 350 (1995); D. Garcia and J. Sola, *Phys. Lett.***354** 335 (1995).

[48] P. Chankowski and S. Pokorski, *Phys. Lett.* **B366**, 188 (1996); W. de Boer, A. Dabelstein, W. Hollik, W. Mosle and U. Schwickerath, Karlsruhe preprint IEKP-KA-96-08, August 1996 (LANL hep-ph/9609209).

Table 2: u Clebsches for models 4(a) and 4(c)

model	u_u	u'_u	u_d	u'_d	u_e	u'_e
a	$-4/3$	$1/3$	-2	-9	-54	3
c	$-4/3$	$1/3$	$2/3$	-9	-54	-1

Table 3: **Model 4 - Results at point II** (see point II on fig. 1a)

Initial parameters: $1/\alpha_G = 24.33$, $M_G = 3.29{\cdot}10^{16}$GeV, ϵ_3 = -4.72% ,

A = 0.734, B = $5.67{\cdot}10^{-2}$, C = $0.865{\cdot}10^{-4}$, E = $1.04{\cdot}10^{-2}$, $\Phi = 1.76$,

$\mu = 80.00$GeV, $m_0 = 700.00$GeV, $M_{1/2} = 240.00$GeV,

$m_{H_d}/m_0 = 1.39$, $m_{H_u}/m_0 = 1.22$, $A_0 = 387.79$GeV, $B\mu$ =120.01GeV^2

Observable	Computed value	Contribution to χ^2	SUSY corrections [in%]
M_Z	91.12	< 0.5	
M_W	80.37	< 0.5	
G_μ	$1.166 \cdot 10^{-5}$	< 0.5	
α_{EM}^{-1}	137.0	< 0.5	1.44
$\alpha_s(M_Z)$	0.1162	< 0.5	12.93
ρ_{new}	$+1.74 \cdot 10^{-4}$	< 0.5	
M_t	173.9	< 0.5	0.75
$m_b(M_b)$	4.360	0.82	5.14
$M_b - M_c$	3.146	1.61	7.90
m_s	162.6	< 0.5	3.68
m_d/m_s	0.0461	< 0.5	0.00
Q^{-2}	0.00173	2.19	1.66
M_τ	1.777	< 0.5	-1.94
M_μ	105.6	< 0.5	-1.46
M_e	0.5113	< 0.5	-1.46
V_{us}	0.2215	< 0.5	0.00
V_{cb}	0.0450	3.79	1.53
V_{ub}/V_{cb}	0.0463	2.84	0.00
$\hat{B}_K$	0.9450	2.10	-3.09
$B(b \to s\gamma)$	$2.388 \cdot 10^{-4}$	< 0.5	
TOTAL χ^2		14.012	

Table 4: **Model 4c - Results at point I** (see point I on fig. 4a)

Initial parameters: $1/\alpha_G = 24.43$, $M_G = 2.50{\cdot}10^{16}$GeV, ϵ_3 = -4.76% ,

A = 0.764, B = $5.26{\cdot}10^{-2}$, C = $1.10{\cdot}10^{-4}$, D = $4.63{\cdot}10^{-4}$, $\delta = 5.70$, E = $1.25{\cdot}10^{-2}$, $\Phi = 1.07$,

$\mu = 80.00$GeV, $m_0 = 400.00$GeV, $M_{1/2} = 280.00$GeV,

$m_{H_d}/m_0 = 1.77$, $m_{H_u}/m_0 = 1.59$, $A_0 = 322.21$GeV, $B\mu = 120.00\text{GeV}^2$

Observable	Computed value	Contribution to χ^2	SUSY corrections [in%]
M_Z	91.12	< 0.1	
M_W	80.34	< 0.1	
G_μ	$1.164 \cdot 10^{-5}$	< 0.1	
α_{EM}^{-1}	136.9	< 0.1	1.25
$\alpha_s(M_Z)$	0.1132	0.93	12.66
ρ_{new}	$+9.87 \cdot 10^{-5}$	< 0.1	
M_t	173.5	< 0.1	0.93
$m_b(M_b)$	4.311	0.22	4.96
$M_b - M_c$	3.499	0.24	6.64
m_s	184.6	< 0.1	4.95
m_d/m_s	0.0496	< 0.1	0.00
Q^{-2}	0.00205	< 0.1	2.01
M_τ	1.776	< 0.1	-4.00
M_μ	105.7	< 0.1	-2.76
M_e	0.5110	< 0.1	-2.76
V_{us}	0.2205	< 0.1	0.00
V_{cb}	0.0406	0.21	2.49
V_{ub}/V_{cb}	0.0744	< 0.1	0.00
$\hat{B}_K$	0.8196	< 0.1	-5.05
$B(b \to s\gamma)$	$2.575 \cdot 10^{-4}$	< 0.1	
TOTAL χ^2		2.039	

Table 5: **Model 4c - Results at point II** (see point II on fig. 4a)

Initial parameters: $1/\alpha_G = 24.36$, $M_G = 3.17{\cdot}10^{16}$GeV, ϵ_3 = -4.89% ,

A = 0.807, B = $5.44{\cdot}10^{-2}$, C = $1.15{\cdot}10^{-4}$, D = $4.94{\cdot}10^{-4}$, $\delta = 5.71$, E = $1.31{\cdot}10^{-2}$, $\Phi = 1.04$,

$\mu = 80.00$GeV, $m_0 = 700.00$GeV, $M_{1/2} = 240.00$GeV,

$m_{H_d}/m_0 = 1.42$, $m_{H_u}/m_0 = 1.24$, $A_0 = 458.35$GeV, $B\mu = 120.66\text{GeV}^2$

Observable	Computed value	Contribution to χ^2	SUSY corrections [in%]
M_Z	91.12	0.02	
M_W	80.38	< 0.02	
G_μ	$1.166 \cdot 10^{-5}$	< 0.02	
α_{EM}^{-1}	137.0	< 0.02	1.43
$\alpha_s(M_Z)$	0.1151	0.34	12.78
ρ_{new}	$+1.87 \cdot 10^{-4}$	0.09	
M_t	175.7	< 0.02	0.74
$m_b(M_b)$	4.287	0.06	5.43
$M_b - M_c$	3.440	0.04	7.56
m_s	189.0	0.03	3.68
m_d/m_s	0.0502	< 0.02	0.00
Q^{-2}	0.00204	< 0.02	1.78
M_τ	1.776	< 0.02	-2.08
M_μ	105.7	< 0.02	-1.50
M_e	0.5110	< 0.02	-1.50
V_{us}	0.2205	< 0.02	0.00
V_{cb}	0.0400	0.07	1.58
V_{ub}/V_{cb}	0.0772	< 0.02	0.00
$\hat{B}_K$	0.8140	< 0.02	-3.18
$B(b \to s\gamma)$	$2.382 \cdot 10^{-4}$	< 0.02	
TOTAL χ^2		0.7306	

Table 6: **Model 4c - Results at point III1** (see point III1 on fig. 4b)

Initial parameters: $1/\alpha_G = 24.51$, $M_G = 3.33{\cdot}10^{16}$GeV, ϵ_3 = -4.34% ,

A = 0.852, B = $5.63{\cdot}10^{-2}$, C = $1.21{\cdot}10^{-4}$, D = $5.06{\cdot}10^{-4}$, $\delta = 5.70$, E = $1.36{\cdot}10^{-2}$, $\Phi = 1.02$,

$\mu = 160.00$GeV, $m_0 = 1400.00$GeV, $M_{1/2} = 170.00$GeV,

$m_{H_d}/m_0 = 1.33$, $m_{H_u}/m_0 = 1.14$, A_0 = -982.43GeV, $B\mu = 123.72\text{GeV}^2$

Observable	Computed value	Contribution to χ^2	SUSY corrections [in%]
M_Z	91.12	0.02	
M_W	80.38	< 0.02	
G_μ	$1.166 \cdot 10^{-5}$	< 0.02	
α_{EM}^{-1}	137.0	< 0.02	1.79
$\alpha_s(M_Z)$	0.1154	0.26	12.89
ρ_{new}	$+1.50 \cdot 10^{-4}$	0.08	
M_t	176.9	0.10	0.62
$m_b(M_b)$	4.275	< 0.02	6.27
$M_b - M_c$	3.429	0.02	8.76
m_s	188.3	0.03	2.85
m_d/m_s	0.0512	< 0.02	0.00
Q^{-2}	0.00203	< 0.02	1.68
M_τ	1.777	< 0.02	-1.41
M_μ	105.7	< 0.02	-0.82
M_e	0.5110	< 0.02	-0.81
V_{us}	0.2205	< 0.02	0.01
V_{cb}	0.0397	0.03	1.62
V_{ub}/V_{cb}	0.0797	< 0.02	0.00
$\hat{B}_K$	0.8000	< 0.02	-3.26
$B(b \to s\gamma)$	$2.311 \cdot 10^{-4}$	< 0.02	
TOTAL χ^2		0.5868	

Table 7: **Model 4c - Results at point III2** (see point III2 on fig. 4c)

Initial parameters: $1/\alpha_G = 24.65$, $M_G = 2.88{\cdot}10^{16}$GeV, ϵ_3 = -4.45% ,

A = 0.888, B = $5.89{\cdot}10^{-2}$, C = $1.23{\cdot}10^{-4}$, D = $5.69{\cdot}10^{-4}$, $\delta = 5.74$, E = $1.40{\cdot}10^{-2}$, $\Phi = 1.02$,

$\mu = 240.00$GeV, $m_0 = 1400.00$GeV, $M_{1/2} = 170.00$GeV,

$m_{H_d}/m_0 = 1.33$, $m_{H_u}/m_0 = 1.14$, A_0 = -1079.39GeV, $B\mu = 128.50\text{GeV}^2$

Observable	Computed value	Contribution to χ^2	SUSY corrections [in%]
M_Z	91.12	< 0.10	
M_W	80.35	< 0.10	
G_μ	$1.165 \cdot 10^{-5}$	< 0.10	
α_{EM}^{-1}	136.9	< 0.10	1.85
$\alpha_s(M_Z)$	0.1124	1.25	12.53
ρ_{new}	$+4.60 \cdot 10^{-5}$	< 0.10	
M_t	176.5	< 0.10	0.61
$m_b(M_b)$	4.306	0.18	9.73
$M_b - M_c$	3.486	0.19	13.45
m_s	178.5	< 0.10	4.09
m_d/m_s	0.0500	< 0.10	0.00
Q^{-2}	0.00203	< 0.10	1.91
M_τ	1.776	< 0.10	-1.93
M_μ	105.7	< 0.10	-1.06
M_e	0.5110	< 0.10	-1.06
V_{us}	0.2205	< 0.10	0.01
V_{cb}	0.0402	0.11	1.73
V_{ub}/V_{cb}	0.0777	< 0.10	0.00
$\hat{B}_K$	0.7949	< 0.10	-3.49
$B(b \to s\gamma)$	$2.269 \cdot 10^{-4}$	< 0.10	
TOTAL χ^2		1.9477	

Table 8: **Model 4c - More Results at points I and II** (see points I and II on fig. 4a) In Higgs sector, we quote all masses with one loop corrections included. For superpartners, masses are at tree level.

For squark and slepton masses, the first two columns are for the third family which are significantly split, while the third and fourth columns are mean values for the nearly degenerate states of the second and first families, respectively.

Observable	Predictions at point I				Predictions at point II			
$m_u/m_d\,\vert_{1GeV}$	0.409				0.440			
$sin^2\theta_W^{(MSSM)}$	0.2342				0.2334			
$sin^2\theta_W^{(SM)}$	0.2323				0.2320			
$\sin 2\alpha$	0.953				0.966			
$\sin 2\beta$	0.513				0.522			
$\sin\gamma$	0.935				0.928			
ρ	-0.120				-0.130			
η	0.316				0.325			
$\tan\beta$	52.77				54.38			
CP even Higgses	73.43	110.81			75.24	110.35		
CP odd Higgs	73.45				75.25			
charged Higgs	115.65				116.92			
gluino	725				630			
charginos	70	260			67	232		
neutralinos	52	95	129	260	48	97	113	232
up squarks	474	614	747	771	487	603	887	905
down squarks	510	552	749	775	513	550	893	909
charged sleptons	66	338	423	448	294	550	716	718
sneutrinos	327		440	440	544		713	714

Table 9: **Model 4c - More Results at points III1 and III2** (see points III1 and III2 on figures 4b and 4c)

Higgs, squark and slepton masses are treated in the same way as for the results quoted on Table VIII.

Observable	Predictions at point III1				Predictions at point III2			
$m_u/m_d\,\vert_{1GeV}$	0.475				0.432			
$sin^2\theta_W^{(MSSM)}$	0.2337				0.2344			
$sin^2\theta_W^{(SM)}$	0.2325				0.2331			
$\sin 2\alpha$	0.973				0.977			
$\sin 2\beta$	0.531				0.516			
$\sin\gamma$	0.925				0.918			
ρ	-0.138				-0.140			
η	0.334				0.323			
$\tan\beta$	55.39				55.86			
CP even Higgses	71.70	112.36			66.70	112.05		
CP odd Higgs	71.70				66.70			
charged Higgs	115.43				112.22			
gluino	447				440			
charginos	101	218			122	274		
neutralinos	62	105	174	217	67	122	251	272
up squarks	558	677	1443	1460	546	666	1440	1458
down squarks	597	641	1459	1462	574	639	1457	1460
charged sleptons	600	1062	1397	1418	564	1051	1397	1418
sneutrinos	1052		1394	1395	1047		1394	1395

Table 10: **Model 4c - Varying the Lower Bound on ϵ_3 at point II** Best fit values of selected GUT parameters and low energy observables are displayed for different lower bounds on ϵ_3. Note that the optimization procedure pushes ϵ_3 to its lower limit. The first line corresponds to the unrestricted case and the corresponding values are taken over from table 5 for the sake of completeness.

ϵ_3	$1/\alpha_G$	$M_G \times 10^{-16}$	A	$\alpha_s(M_Z)$	$G_\mu \times 10^5$	M_{top}	$m_b(M_b)$	χ^2_{total}
-4.89%	24.362	3.17	0.807	0.1151	1.166	175.7	4.287	0.731
-3.00%	24.628	2.10	0.808	0.1154	1.161	176.1	4.291	0.959
-2.00%	24.767	1.69	0.802	0.1156	1.159	176.1	4.295	1.279
-1.00%	24.907	1.37	0.813	0.1158	1.157	176.6	4.295	1.694
0.00%	25.044	1.11	0.818	0.1160	1.155	177.0	4.296	2.244
$+1.00\%$	25.177	0.89	0.794	0.1162	1.153	176.4	4.304	2.944
$+2.00\%$	25.314	0.73	0.810	0.1164	1.151	177.1	4.302	3.675
$+3.00\%$	25.450	0.59	0.827	0.1166	1.149	177.9	4.303	4.583
$+4.00\%$	25.578	0.48	0.797	0.1167	1.147	177.1	4.309	5.534

Table 11:

Model 4c - Sensitivity of the results of table 10 to the magnitude of the theoretical uncertainties In comparison to table 10, the best fit values of the same GUT parameters and low energy observables are displayed for different lower bounds on ϵ_3, but this time for the uncertainty σ=0.1% for M_Z, G_μ and α_{em}, and the experimental value σ=130MeV for M_W. (σ=0.5% for M_Z, M_W and α_{em}, and σ=1.0% for G_μ was assumed in table 10, as well as throughout this paper.) The first line corresponds to the case when ϵ_3 is unrestricted.

ϵ_3	$1/\alpha_G$	$M_G \times 10^{-16}$	A	$\alpha_s(M_Z)$	$G_\mu \times 10^5$	M_{top}	$m_b(M_b)$	χ^2_{total}
-5.36%	24.295	3.53	0.807	0.1150	1.166	175.6	4.286	1.20
-3.00%	24.494	2.55	0.808	0.1186	1.165	177.4	4.418	7.49
-2.00%	24.579	2.21	0.803	0.1201	1.165	177.9	4.471	13.97
0.00%	24.759	1.64	0.818	0.1229	1.164	179.6	4.560	34.02

FIGURE CAPTIONS

Figure 1.
Model 4 global analysis results in the $m_0 - M_{1/2}$ plane, for a fixed value of the Higgs parameter
a) $\mu(M_Z) = 80$ GeV ,
b) $\mu(M_Z) = 160$ GeV ,
c) $\mu(M_Z) = 240$ GeV .
Solid (dashed, double-dash-dotted) lines represent contour lines of constant $\chi^2 = 15$ (14,13) / 5dof. The star on figure 1a marks the point (m_0=700GeV, $M_{1/2}$=240GeV). In the text it is referred to as point II and the corresponding results obtained at this point are listed in table 3.

Figure 2.
Results for Model 4 with one observable removed from the χ^2 function (the corresponding standard deviation of that observable is inflated by a large factor), at fixed values of the Higgs parameter $\mu(M_Z)$=80GeV and $M_{1/2}$=240GeV. Eight observables tried, (and their values obtained at the minimum of χ^2) are as follows: α_s (0.1144) - dots, $BR(b \to s\gamma)$ ($2.29 \cdot 10^{-2}$) - diamonds, $M_b - M_c$ (2.84GeV) - solid squares, $1/Q^2$ ($1.50 \cdot 10^{-3}$) - open circles, V_{ub}/V_{cb} (0.045) - triangles, $m_b(M_b)$ (4.68GeV) - stars, B_K (1.12) - open squares, V_{cb} (0.0465) - solid circles. For comparison, the thick solid line represents the best χ^2 values of Model 4 with all observables present with their regular standard deviations as quoted in table 1. No significant improvement of Model 4 is observed. Recall that leaving out an observable from the χ^2 function means reducing the number of degrees of freedom by one.

Figure 3.
Model 4a global analysis results in the $m_0 - M_{1/2}$ plane, for a fixed value of the Higgs parameter
a) $\mu(M_Z) = 80$ GeV ,
b) $\mu(M_Z) = 160$ GeV ,
c) $\mu(M_Z) = 240$ GeV .
Solid (dashed, double-dash-dotted) lines represent contour lines of constant $\chi^2 = 6$ (4,3) / 3dof.

Figure 4.
Model 4c global analysis results in the $m_0 - M_{1/2}$ plane, for a fixed value of the Higgs parameter
a) $\mu(M_Z) = 80$ GeV ,
b) $\mu(M_Z) = 160$ GeV ,
c) $\mu(M_Z) = 240$ GeV .
Solid (double-dash-dotted, dotted) lines represent contour lines of constant $\chi^2 = 6$ (3,1) / 3dof. The stars mark the points (400,280), (700,240) and (1400,170). In the text, these are referred to as points I, II, III1 (point III at μ=160GeV) and III2 (point III at μ=240GeV). The

corresponding results and predictions obtained at these points are listed in tables 4 through 9.

Figure 5.
Stability of the predictions for sin2α and sin2β, the parameters of the unitarity triangle. "x" symbols denote the points predicted by
a) model 4c ,
b) model 4a
at those regions in the SUSY parameter space where $\chi^2 < 3$ / 3dof . Dots in the figures represent the boundary of the allowed region resulting from a combined general Standard Model fit [44] for $f_{B_d} = 200 \pm 40 MeV$, $B_{B_d} = 1.0$, $\hat{B}_K = 0.75 \pm 0.10$.

Figure 6a.
The dependence of the quality of the fit on the GUT threshold correction ϵ_3, in model 4c. The thick solid line represents the results of model 4c with ϵ_3 unrestricted. The dotted line constrains ϵ_3 to be positive (and the optimization procedure always settles ϵ_3 very close to zero). Curves with solid squares, open circles and stars correspond to the results of the optimization performed with negative lower limit on ϵ_3 -3%, -2% and -1%, respectively. Curves with open triangles, solid circles, open squares and solid triangles correspond to the cases with lower bound on ϵ_3 greater than zero, namely 1%, 2%, 3% and 4%, respectively. In all cases the optimization procedure tends to yield the values of ϵ_3 very close to the lower bound. Table 10 displays the effect of different ϵ_3 lower bounds on various GUT parameters and low energy observables at point II (i.e. at m_0=700GeV).

Figure 6b.
The same as in figure 6a, with a tighter theoretical uncertainty on precisely measured electroweak observables. In this figure the uncertainty for M_Z, G_μ and α_{em} is set to 0.1% and the actual experimental error 130MeV is assigned to $\sigma(M_W)$; as opposed to the uncertainty of 0.5% for M_Z, M_W and α_{em}, and $\sigma(G_\mu)$=1.0% , assumed in figure 6a. As before, in all restricted cases the optimization procedure tends to yield the values of ϵ_3 very close to the lower bound. Table 11 displays the effect of different ϵ_3 lower bounds on various GUT parameters and low energy observables at point II (i.e. at m_0=700GeV).

Figure 7.
The variation of the quality of the fit for different lower bounds on tree level pseudoscalar mass, in model 4c. The thick solid line represents the results of model 4c with m_A^{tree} >80GeV. When very close to this limit, the pseudoscalar mass receives negative corrections, and its one loop corrected value turns out to be at the experimental limit (see tables 8 and 9 for the results at point m_0=700GeV). Curves with solid and open circles, solid squares, and stars correspond to the lower limit on m_A^{tree} of 130GeV, 200GeV, 300GeV and 500GeV, respectively.

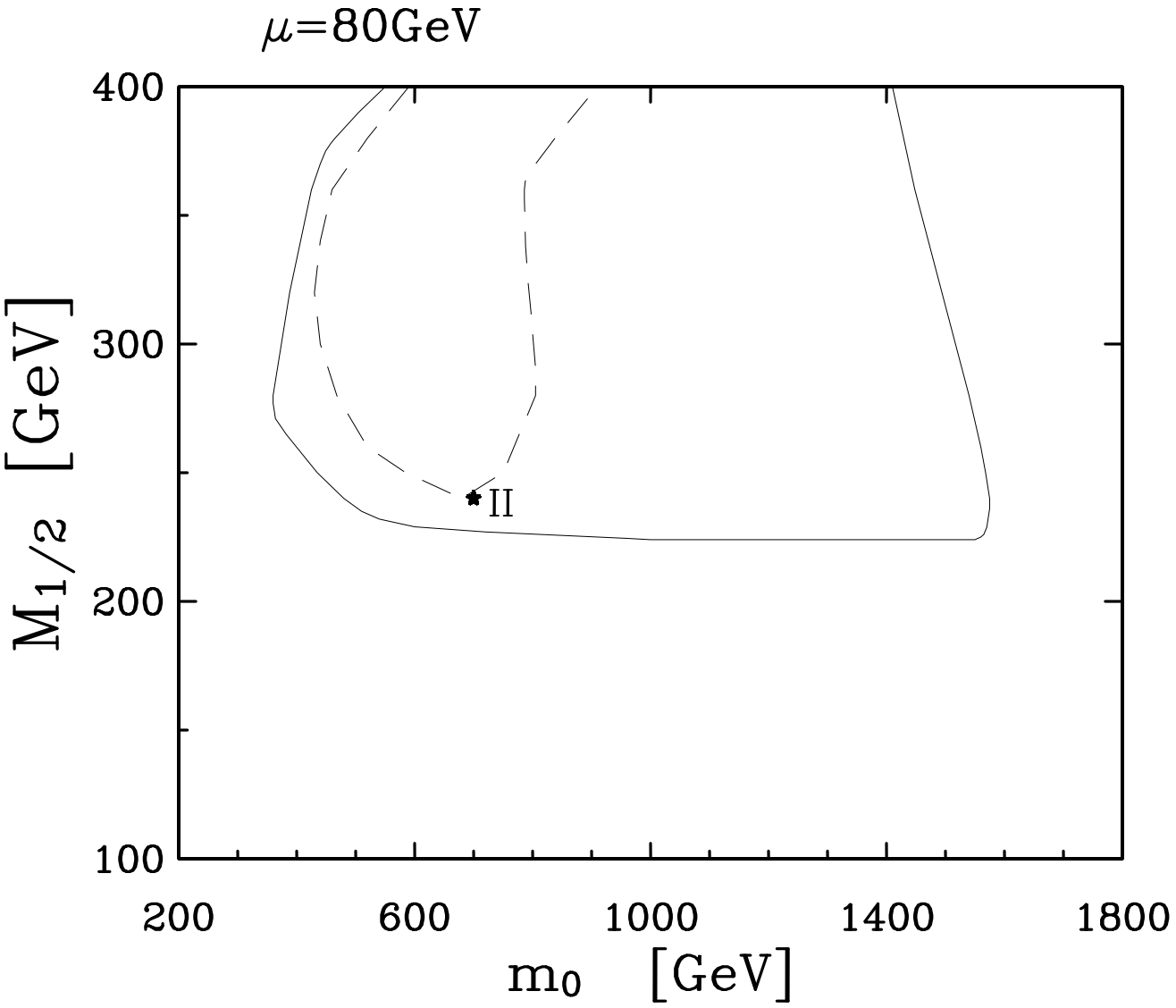

μ=80GeV
400
300
200
100
$M_{1/2}$ [GeV]
II
200
600
1000
1400
1800
m_0 [GeV]

Figure 1a

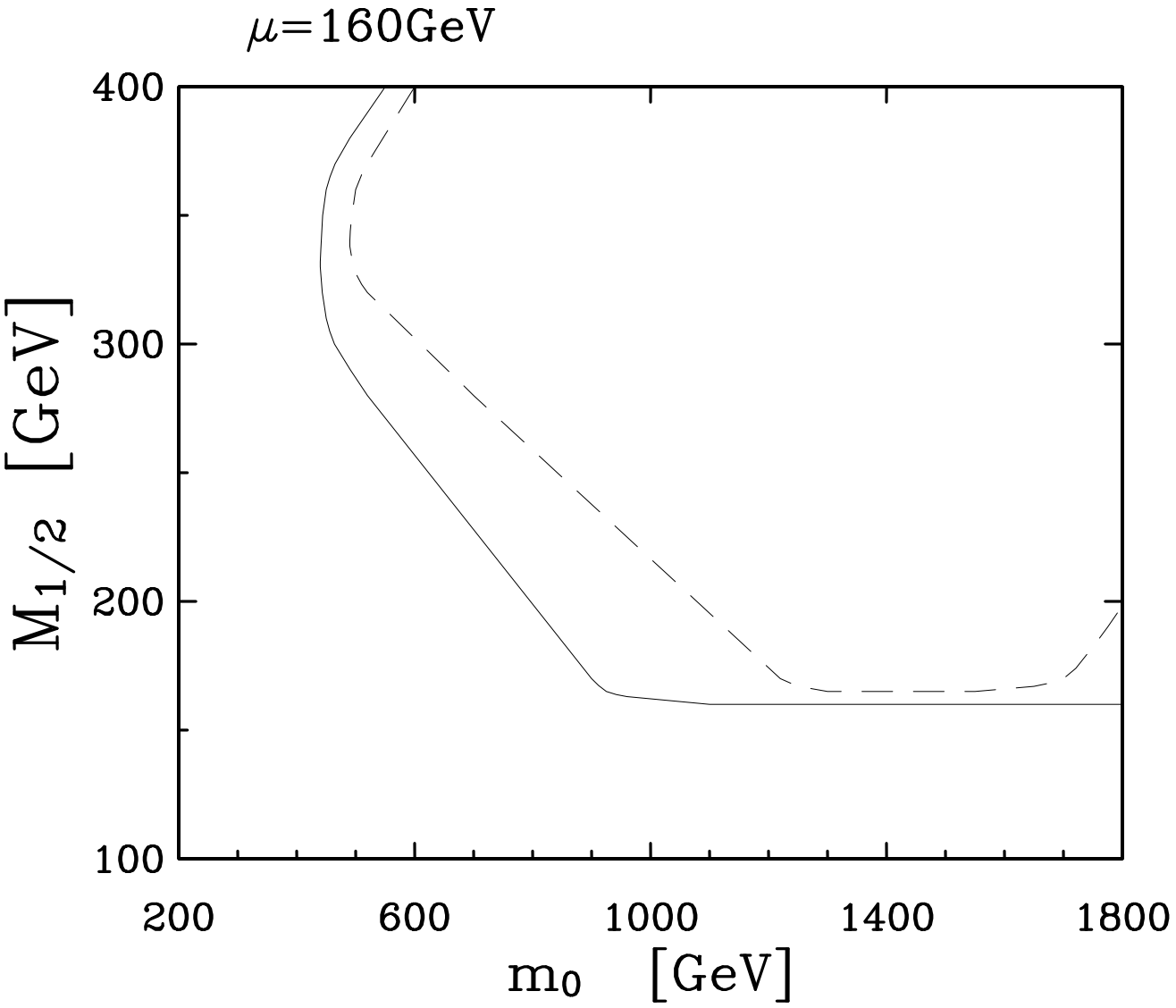


Figure 1b

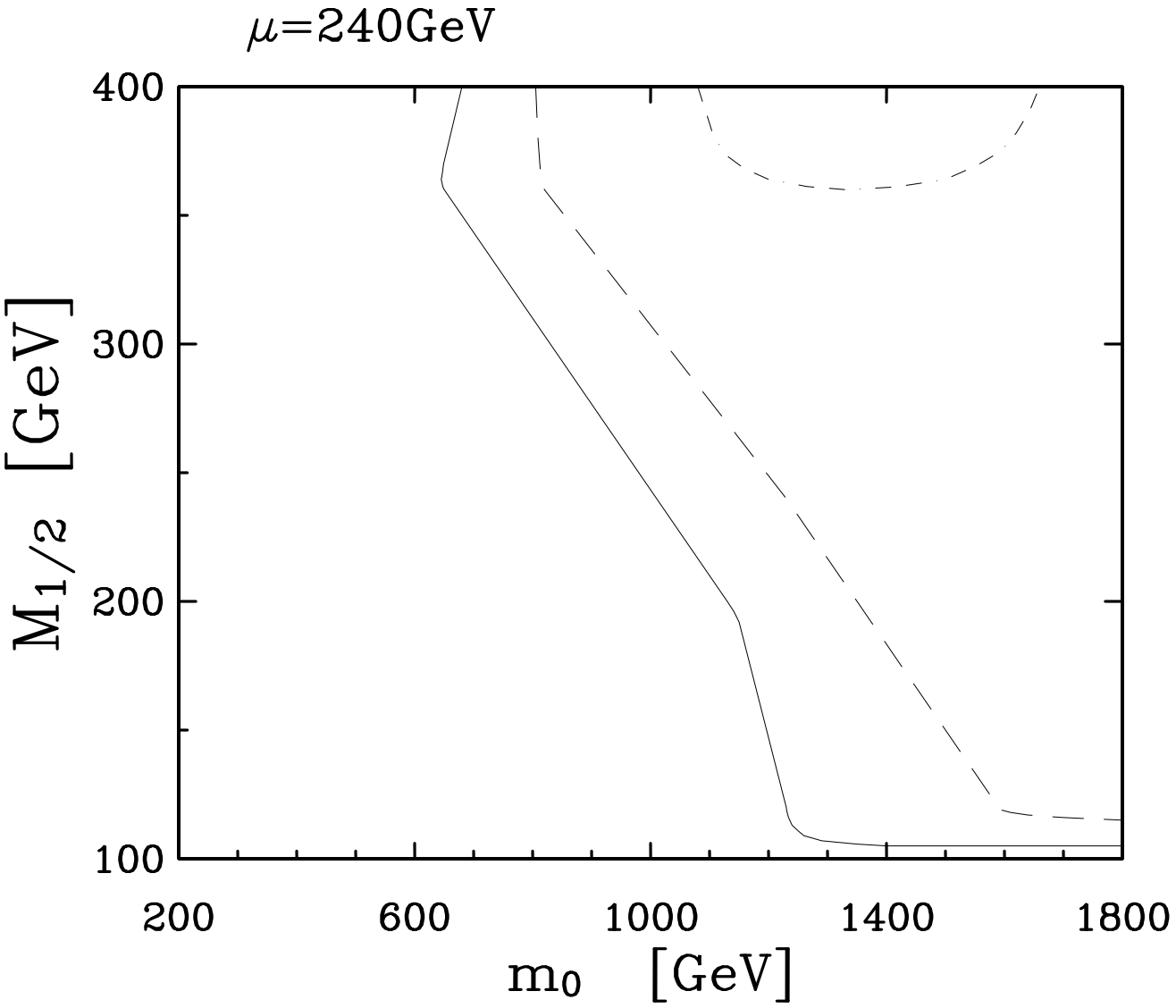


Figure 1c

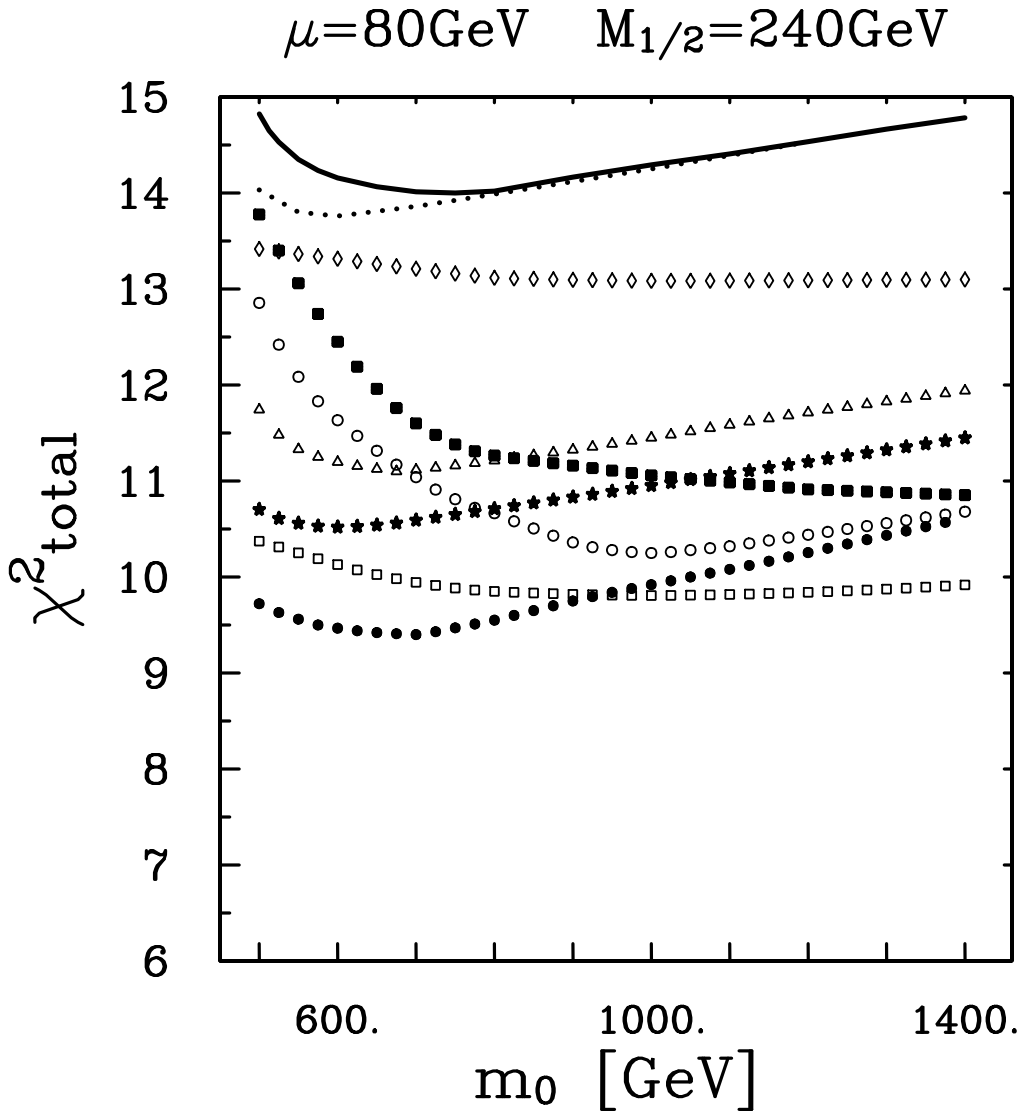

μ=80GeV M1/2=240GeV
15
14
13
12
11
10
9
8
7
6
χ2total
600.
1000.
1400.
m0 [GeV]

Figure 2

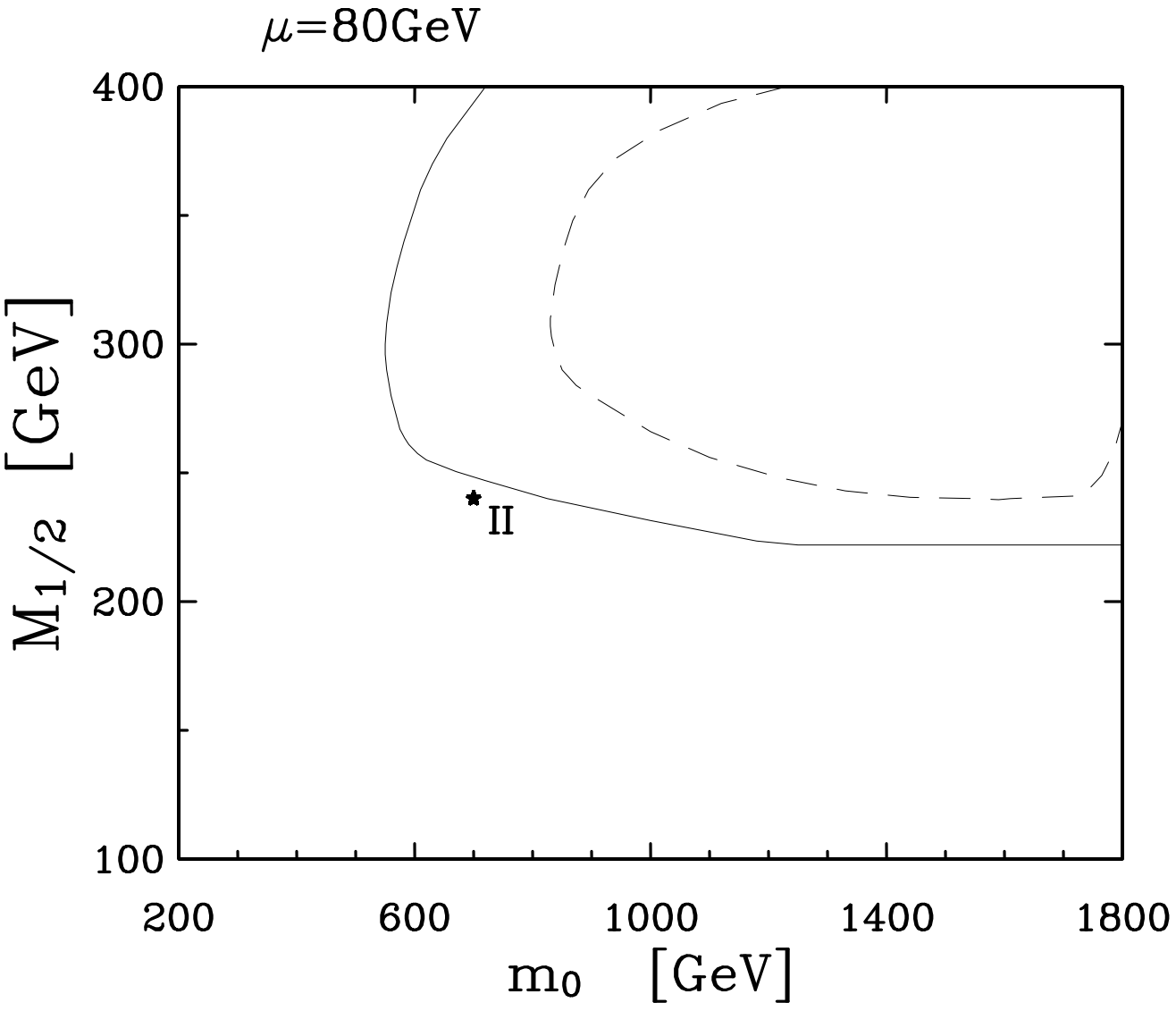

μ=80GeV
400
300
200
100
$M_{1/2}$ [GeV]
II
200
600
1000
1400
1800
m_0 [GeV]

Figure 3a

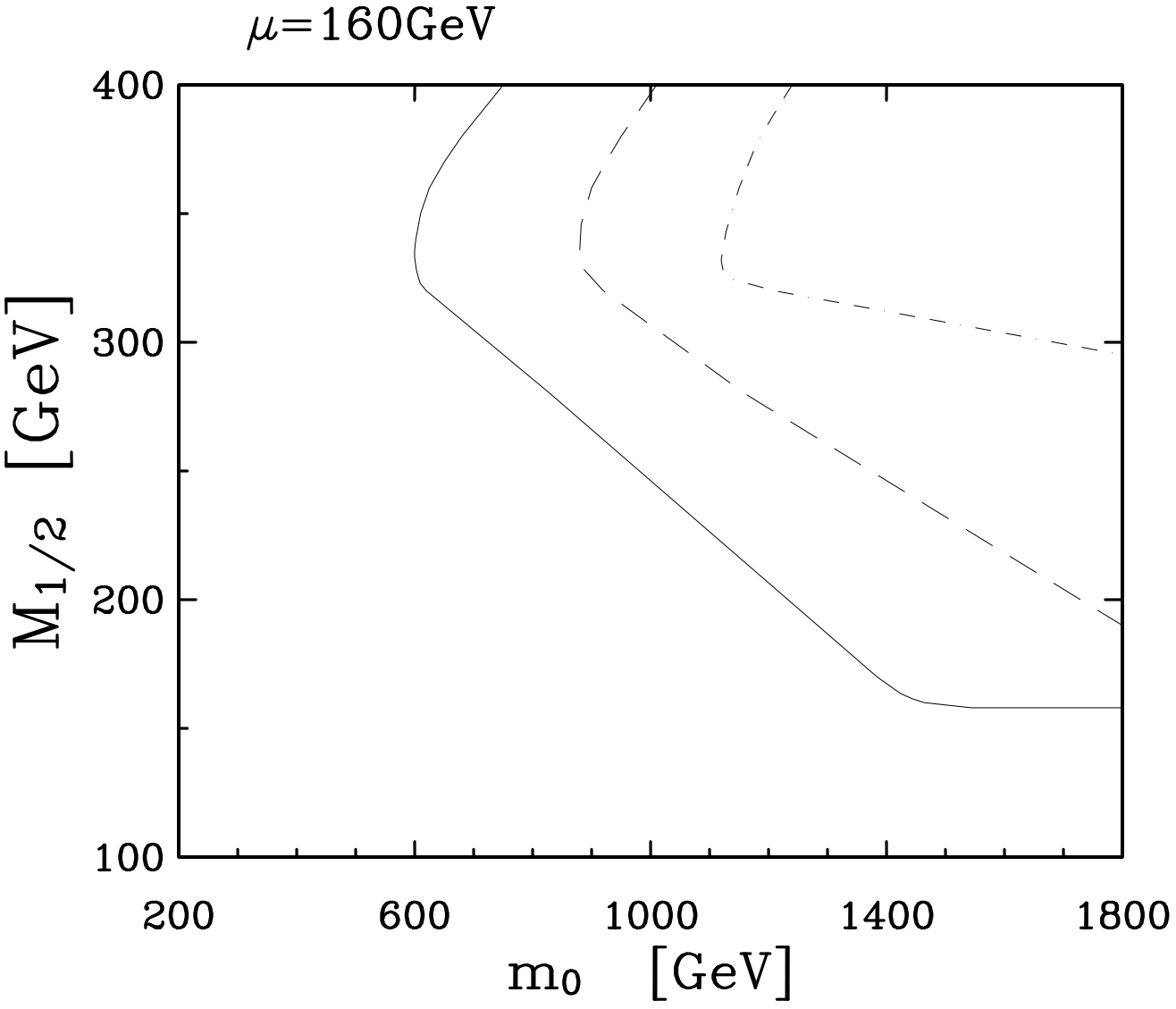


Figure 3b

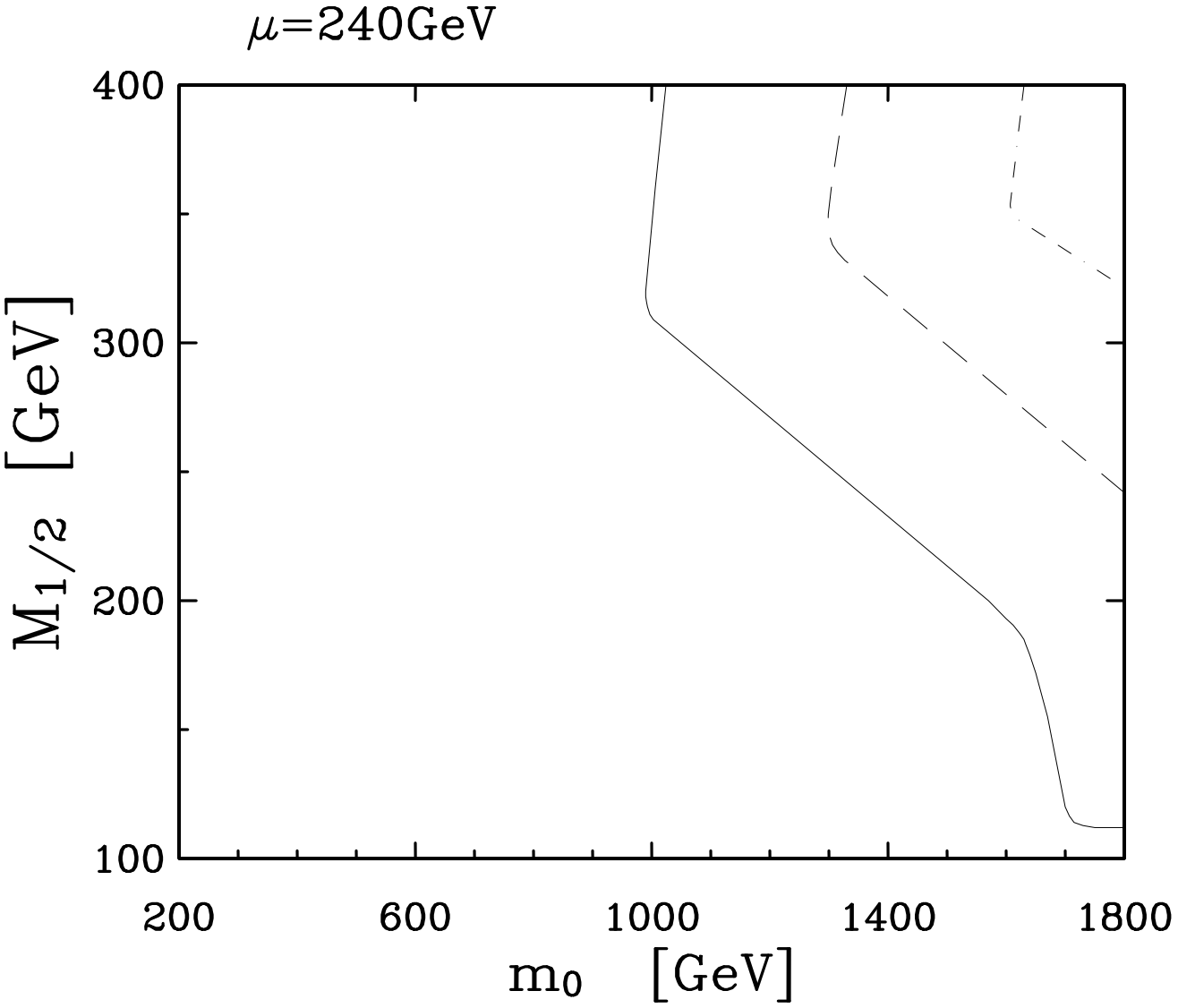


Figure 3c

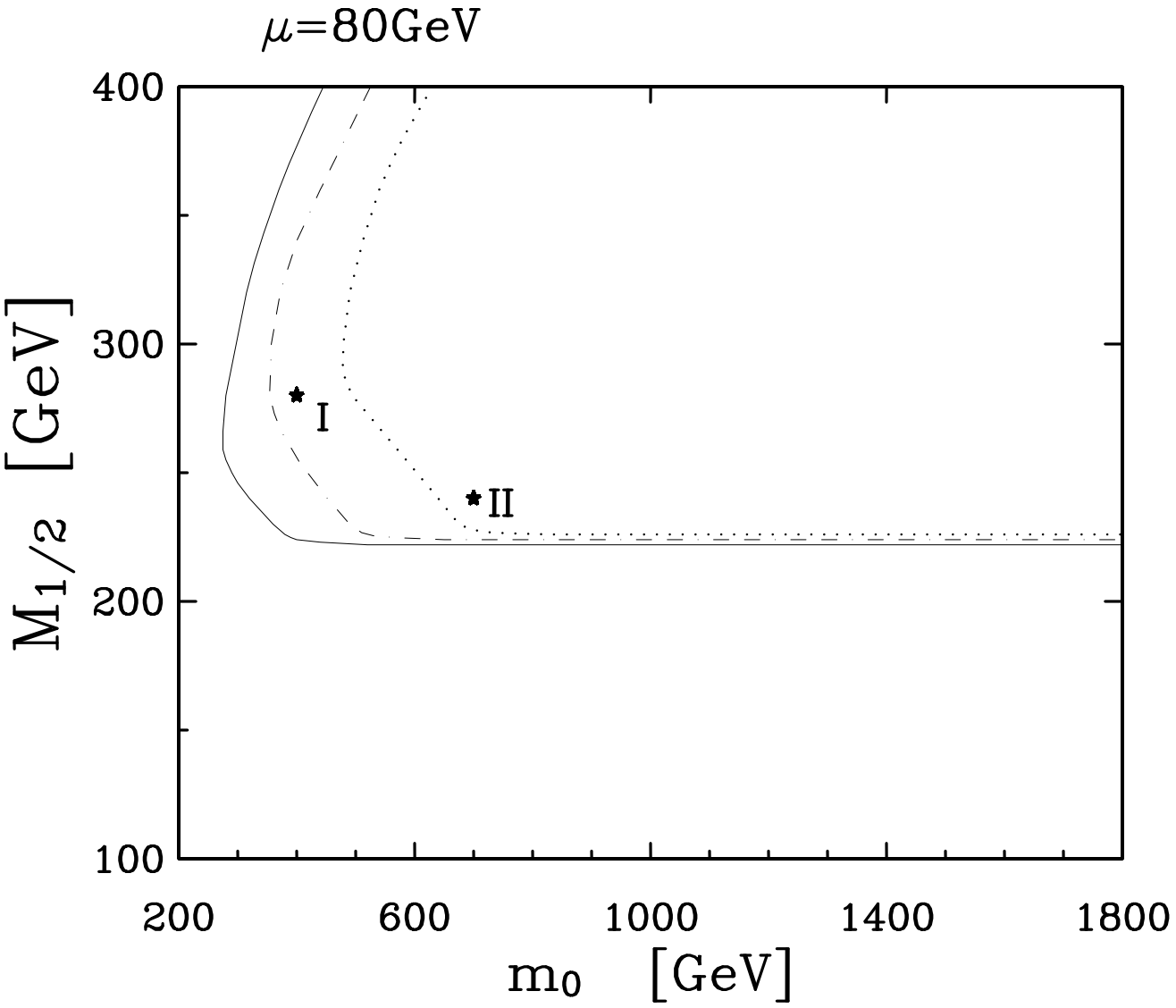

μ=80GeV
400
300
200
100
M1/2 [GeV]
I
II
200
600
1000
1400
1800
m0 [GeV]

Figure 4a

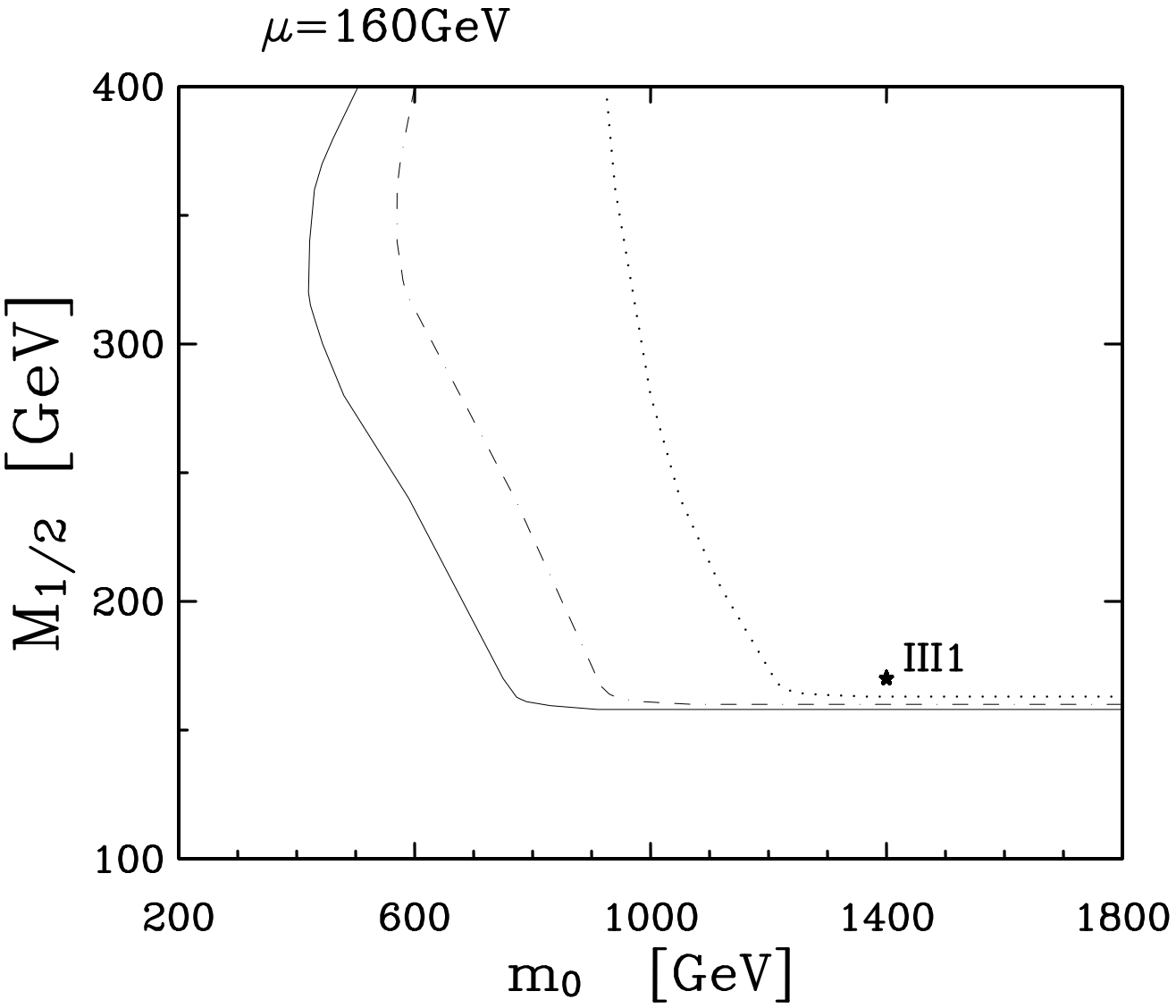

μ=160GeV
400
300
200
100
M1/2 [GeV]
III1
200
600
1000
1400
1800
m0 [GeV]

Figure 4b

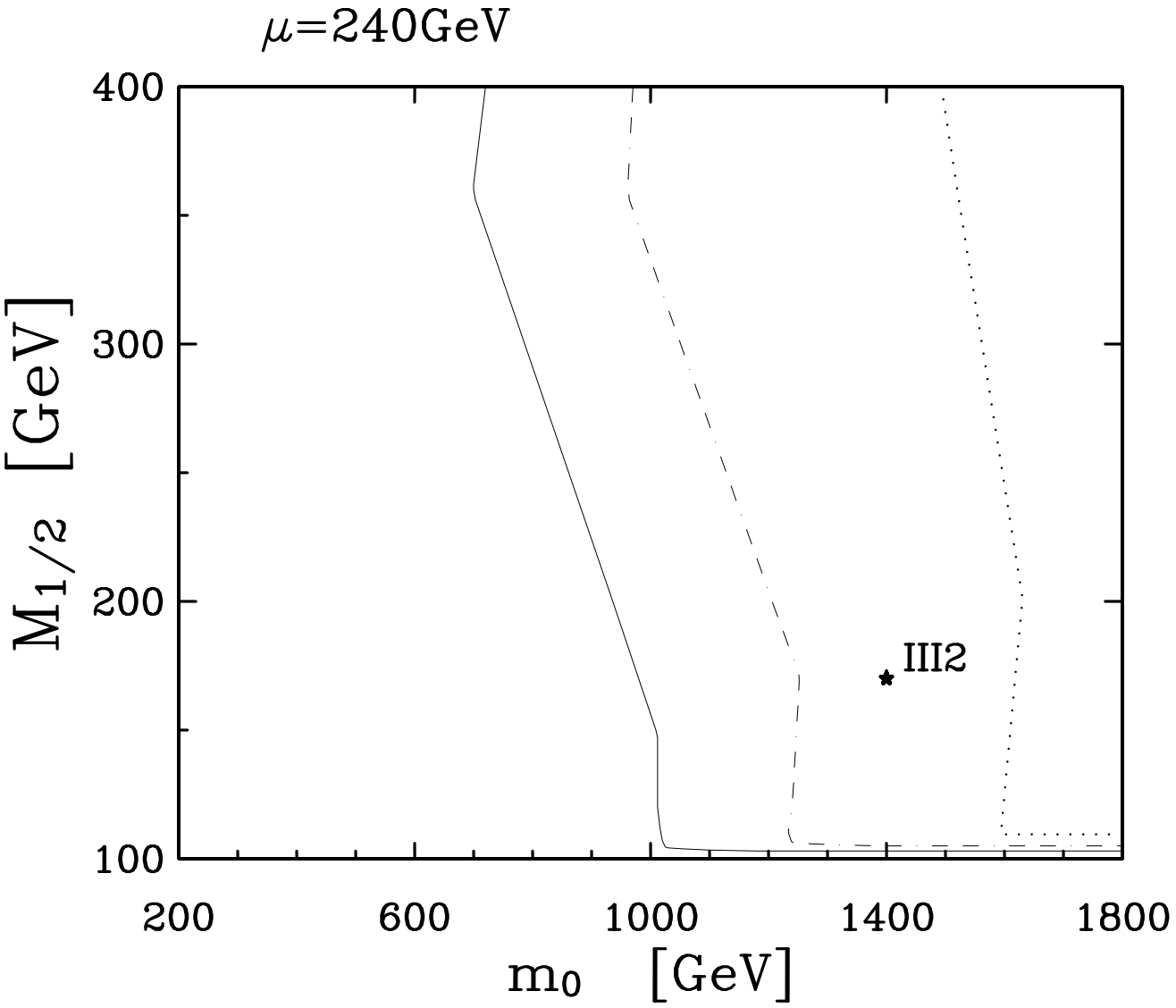

μ=240GeV
400
300
200
100
$M_{1/2}$ [GeV]
III2
200
600
1000
1400
1800
m_0 [GeV]

Figure 4c

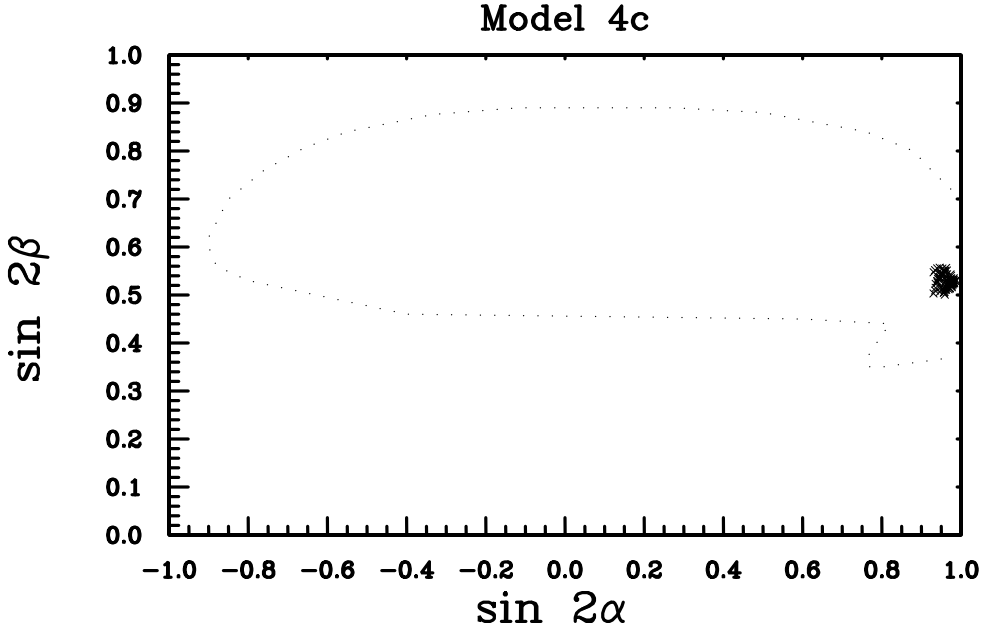


Figure 5a

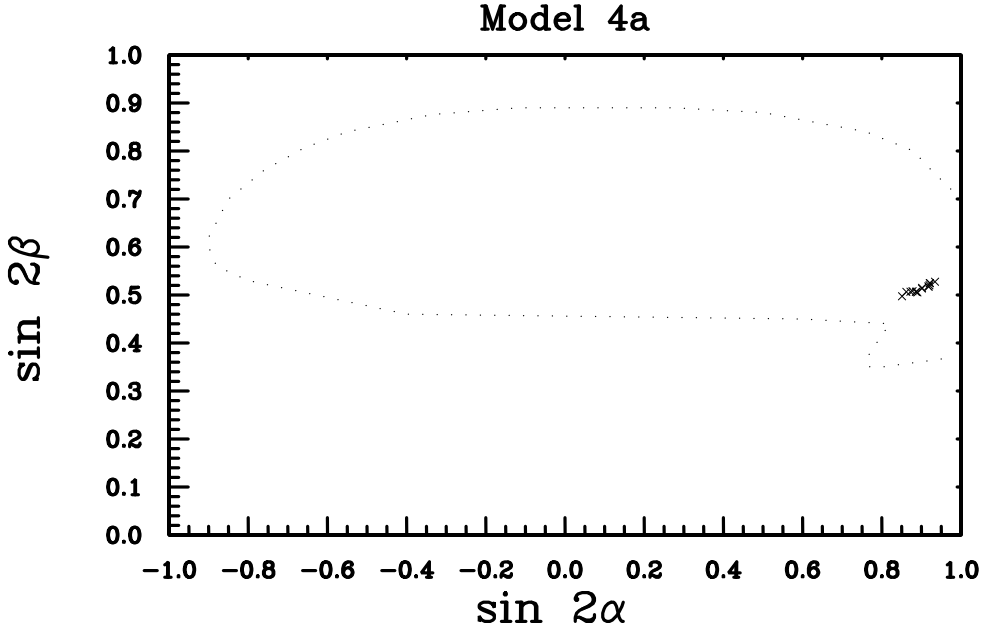


Figure 5b

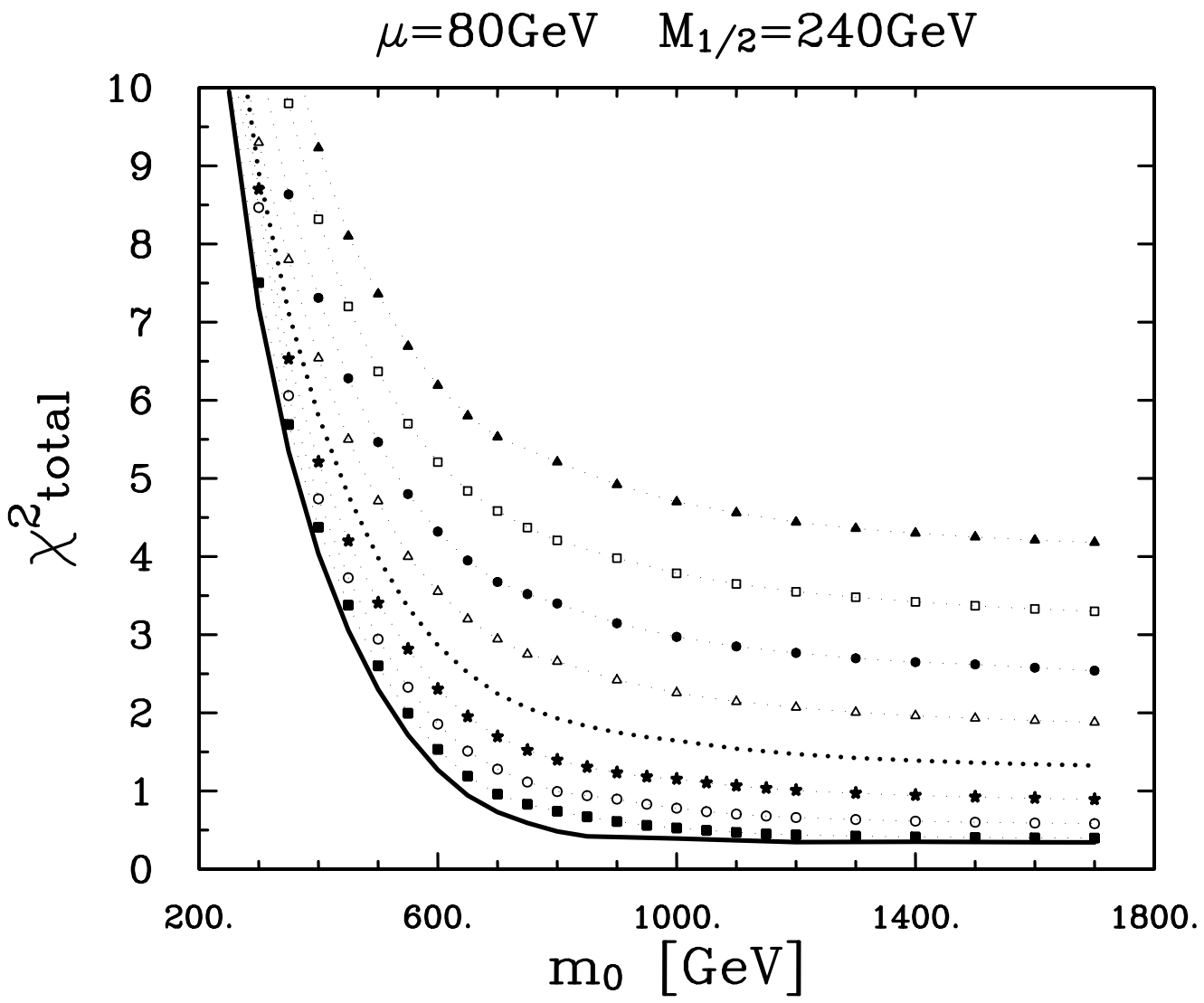

μ=80GeV $M_{1/2}$=240GeV
χ^2_{total}
0
1
2
3
4
5
6
7
8
9
10
200.
600.
1000.
1400.
1800.
m_0 [GeV]

Figure 6a

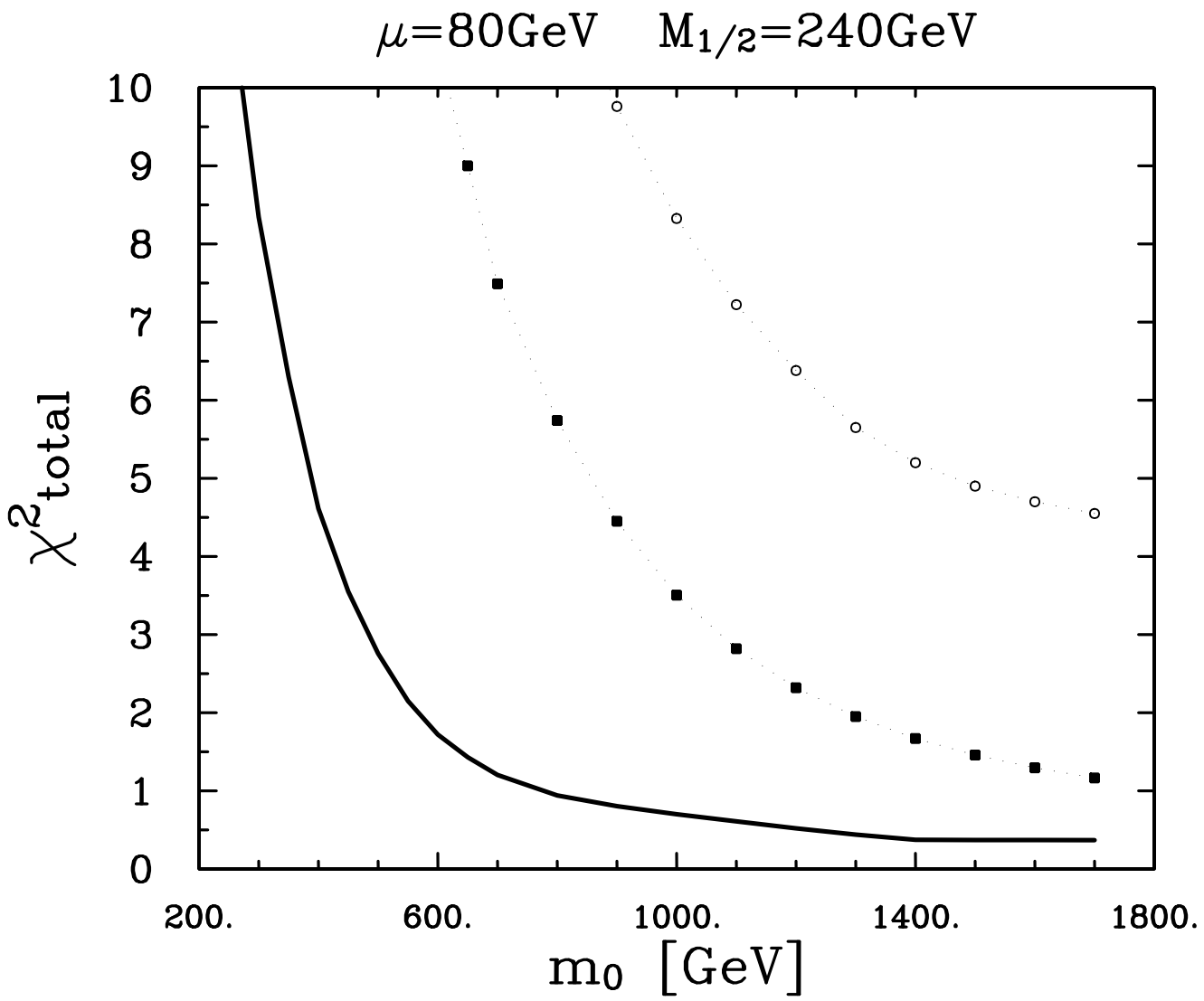

μ=80GeV M1/2=240GeV
χ2total
m0 [GeV]
0
1
2
3
4
5
6
7
8
9
10
200.
600.
1000.
1400.
1800.

Figure 6b

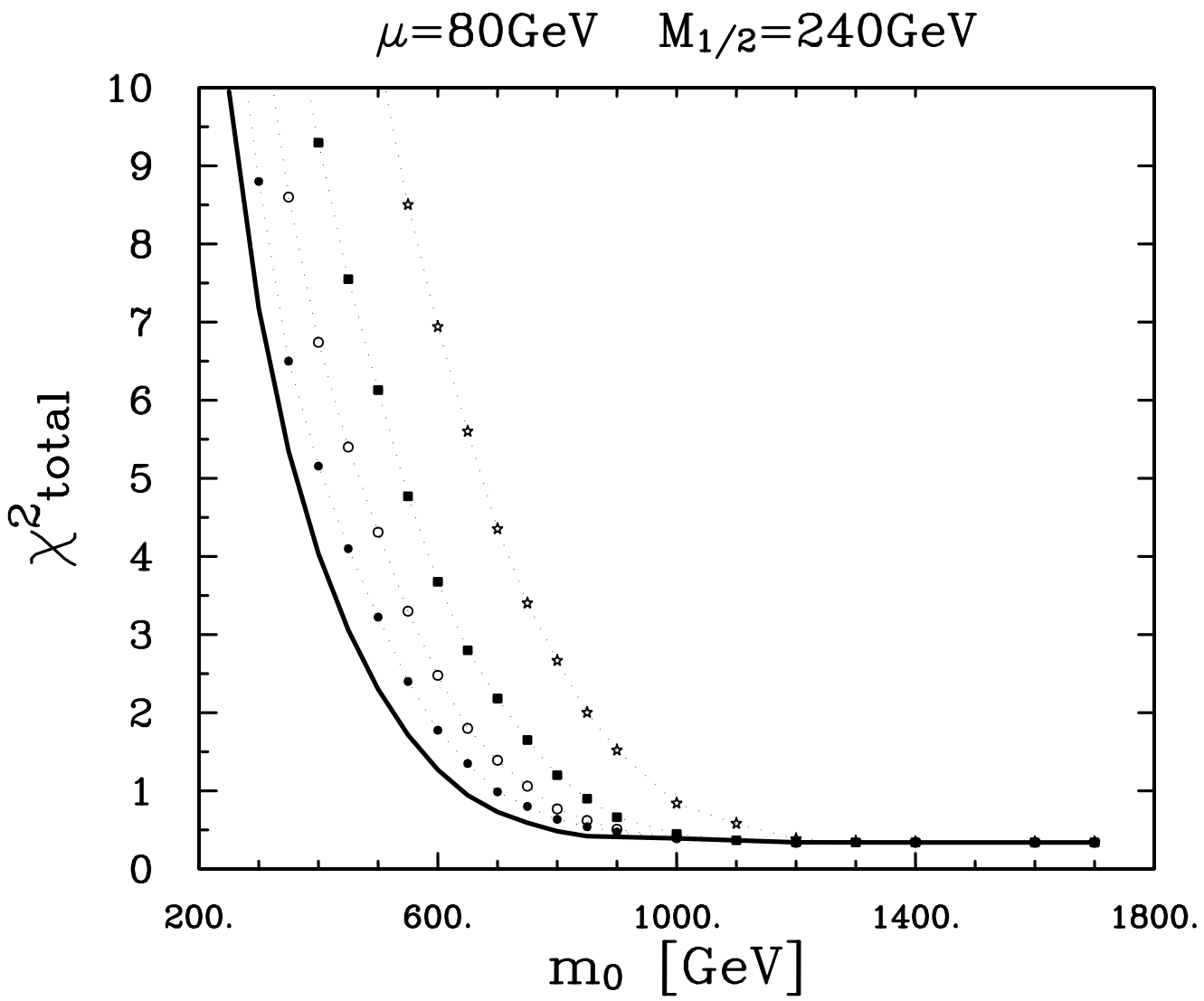

μ=80GeV $M_{1/2}$=240GeV
χ^2_{total}
0
1
2
3
4
5
6
7
8
9
10
200.
600.
1000.
1400.
1800.
m_0 [GeV]

Figure 7